

Gallium interstitial contributions to diffusion in gallium arsenide

J. T. Schick*

Physics Department, Villanova University, Villanova, Pennsylvania 19085

C. G. Morgan and P. Papoulias

*Department of Physics and Astronomy,
Wayne State University, Detroit, Michigan 48202*

(Dated: November 15, 2018)

Abstract

Enthalpies of formation of gallium interstitials and all the other native point defects in gallium arsenide are calculated using the same well-converged *ab initio* techniques. Using these results, equilibrium concentrations of these defects are computed as a function of chemical potential from the arsenic rich limit to the gallium rich limit and as a function of the doping level from *p*-type to *n*-type. Gallium interstitial diffusion paths and migration barriers for diffusion are determined for all the interstitial charge states which are favored for Fermi levels anywhere in the gap, and the charge states which dominate diffusion as a function of Fermi level are identified. The effects of chemical potential, doping level, and non-equilibrium defect concentrations produced by ion implantation or irradiation on gallium self-diffusion are examined. Results are consistent with experimental results across the ranges of doping and stoichiometry where comparisons can be made. Finally, these calculations shed some light on the complex situation for gallium diffusion in gallium arsenide that is gallium-rich and doped heavily *p*-type.

PACS numbers: 61.72.Bb, 71.55.Eq, 66.30.Dn, 66.30.H-

I. INTRODUCTION

Gallium arsenide is used in numerous applications in which converting between electrical energy and light is important, and is therefore an important material of continuing technological interest. The successful operation of gallium-arsenide-based devices generally depends on their structure of layers of varying composition and/or doping, and the interfaces between these layers. The motions of native, iso-electronic substituent, and dopant atoms are manipulated during growth and fabrication to produce the desired atomic composition in each region. After fabrication, the potential for continued movement of these atoms must be understood and controlled to avoid degradation of performance and eventual device failure.

Native defects such as interstitials, vacancies, and antisites are often electrically active, and can strongly affect device characteristics and longevity. Motion of native point defects, such as vacancies and interstitials produced by non-stoichiometric growth or irradiation at the surface, can lead to formation of voids, interstitial clusters, precipitates, and other extended defects, as well as altered spatial profiles of the point defects. The processes involving motion of the native point defects which control self-diffusion are often important for diffusion of foreign atoms as well.

The diffusion properties of a particular native defect are determined by the energy barriers for migration of that defect along its potential pathways. When these energy barriers are combined with the concentration of the defect in the material and the potential for interaction with foreign atoms, the likelihood of this particular defect to enhance both self-diffusion and the diffusion of the foreign atoms can be estimated. Native defects outside the crystal lattice, such as interstitials, generally possess lower migration barriers than defects on the lattice, such as vacancies.¹ Although much experimental and theoretical work has been done to determine and characterize the most important microscopic mechanisms for gallium interstitial diffusion in gallium arsenide, there are still gaps in the current overall picture of gallium interstitial diffusion in this material.

Self-diffusion is more difficult to examine experimentally than foreign atom diffusion because concentrations of the native species may be nearly uniform across the sample, and looking at these concentrations cannot identify the individual motions of the identical atoms. Calculations fit to the experimental results for the simultaneous diffusion of two species, for example interdiffusion of gallium and aluminum at an interface between gallium arsenide and aluminum gallium arsenide, require that a reasonably simple model with a small number of fitting parameters is sufficient to describe the experimental situation. However, studies of the broadening of boundary layers in multi-layered structures of gallium arsenide and aluminum gallium arsenide have been extensively used to investigate diffusion of gallium and aluminum in $\text{Al}_x\text{Ga}_{1-x}\text{As}$.^{1,2} More direct methods for determining diffusion barriers for self-diffusion may use material grown or implanted with an isotope tracer in one region. After annealing and subsequent measurement of the spatial dependence of the isotope concentrations as a function of annealing time, temperature, and Fermi level, theoretical model calculations are fitted to the observed concentration profiles,¹ and these fits are used to generate numerical values for the formation and migration energies of the defects that are assumed to dominate the diffusion under the existing experimental conditions. In some cases, one model is proposed and shown to fit the experimental results,³ and in other cases, more than one alternative model is found which can fit the experimental results.⁴

Initially, gallium interstitial diffusion was proposed to be modeled well with doubly or triply positive charge states.² This proposal was supported by early analyses of diffusion

experiments involving zinc and cadmium, which are both known to be substitutional p -type dopants in the gallium sublattice.² Zucker *et al.* studied the effects of ion-implanted zinc on the boundary profiles of superlattices of gallium arsenide and aluminum gallium arsenide and drew the conclusion that gallium interstitials were diffusing in a doubly or triply positive charge state.⁵ Bösker *et al.* diffused zinc into gallium arsenide under arsenic rich conditions⁶ and cadmium into gallium arsenide under arsenic rich and arsenic poor conditions,⁷ and also concluded that the doubly and triply positive charge states of gallium interstitials can adequately model the diffusion profiles.^{6,7}

However, in a later study employing isotope heterostructures with an implanted dopant to determine the relationship between zinc and gallium diffusion in gallium arsenide⁸ it was proposed that it is the neutral charge state of the gallium interstitial and the neutral and singly-positive charge states of the gallium vacancy that are important in zinc-gallium co-diffusion, contrasting with the earlier studies on interstitials. In subsequent work, Bracht *et al.*³ examined zinc and gallium co-diffusion into the surface of gallium arsenide, further refining their conclusion that the diffusion profiles can be fitted successfully by requiring that the gallium interstitials which contribute to diffusion are in a neutral or singly-positive charge state. It should be noted that using a zinc gallium alloy as a source for the indiffusing atoms in these experiments means the material is being prepared both gallium rich and p -type. However, the authors state that only samples with sufficiently low levels of zinc at the surface are kept for analysis.³ This has the effect of avoiding heavy p -type doping. The authors in Refs. 3 and 8 conclude from their own measurements and from re-analysis of the results of Bösker^{6,7} that interstitial gallium in the neutral and singly positive charge states are partial contributors to gallium diffusion, with gallium vacancies contributing more strongly over much of the experimentally accessible range of stoichiometry and doping level. Under arsenic-rich conditions, these authors observe an enhanced contribution of gallium vacancies to gallium diffusion. Finally, under gallium-rich conditions in heavily- p -doped material, the authors have yet to determine a model that properly fits the diffusion profile.^{3,9} This complex situation requires a comprehensive theoretical picture capable of addressing the numerous defect configurations and charge states that may contribute significantly to the diffusion.

In an early computational effort that included a wide range of potentially important defects in gallium arsenide, Zhang and Northrup used first-principles methods to calculate the formation energies for antisites, tetrahedral interstitials, and vacancies of the native atoms as a function of doping from p -type to n -type and as a function of chemical potential across the range from arsenic-rich to gallium-rich.¹⁰ They concluded that gallium self-diffusion in n -type arsenic-rich gallium arsenide would be dominated by gallium vacancies, while in the p -type gallium-rich limit, gallium interstitials in a highly-positive charge state would dominate diffusion.¹⁰ Since the time of this study, computing power has substantially increased, relaxing restrictions on the size of supercells and the accuracy of approximations for the sum over all occupied states which can be achieved, thus allowing more accurate calculations of the properties of isolated point defects. Advances in computer power and program development have also expanded the number of possible starting configurations that can be studied, and enhanced theorists' ability to explore the potential energy surface in the vicinity of these configurations. It has been shown that lower-symmetry interstitials often have comparable or lower energies of formation than high-symmetry, tetrahedral interstitials.¹¹ For example, $\langle 110 \rangle$ split interstitials have a lower energy of formation than tetrahedral interstitials both for arsenic interstitials in gallium arsenide¹²⁻¹⁴ and for silicon interstitials in silicon¹⁵⁻¹⁸ over a significant range of Fermi levels in the gap.

In addition to the exploration of lower symmetry defects, several thorough convergence studies for defect calculations have also been performed.^{14,19,20} For example, it was shown that the smaller supercells and smaller number of k -points in sums over k -space which were used in earlier calculations result in errors ranging from several tenths of eV to well over an eV in calculations of the defect formation and ionization energies for arsenic interstitials in gallium arsenide.¹⁴ Later calculations using the larger supercells and larger number of k -points which are required for convergence have concluded that tetrahedral interstitial configurations are the most energetically favorable for gallium interstitials in gallium arsenide, and have also investigated lower symmetry configurations which may be important intermediate points along low-energy diffusion paths.²¹ Most recently, all the simple intrinsic defects in gallium arsenide have been examined with a single approach, including the most thorough study to date of convergence and the effects of using different density functionals (local density and generalized gradient approximation).²⁰

Following these recent advances in calculational accuracy and the ability to consider diffusion paths without restriction to paths of high symmetry, *ab initio* studies of the diffusion of gallium and arsenic vacancies²²⁻²⁴ and arsenic interstitials²⁵ in gallium arsenide have been carried out. In recent *ab initio* studies of the diffusion of gallium interstitials in gallium arsenide,^{26,27} the migration barriers for gallium interstitials in gallium arsenide in the neutral and singly positive charge states have been calculated, and the resulting computed migration activation enthalpies for interstitials in these two charge states were found to be comparable to the migration activation enthalpies obtained from recent models fit to experiments.³ These computed migration activation enthalpies for gallium interstitials in the neutral and singly positive charge states²⁶ were actually 0.5 eV lower than the experimental values³ to which they were compared, which as the authors noted may be due to a number of reasons, ranging from the finite scaling correction used in the theory (for non-zero charge state migrations) and the lack of thermal or entropic effects in the theoretical calculations to assumptions made in the model calculations used for analysis of the experiment and assumptions about the material preparation used when comparing the theoretical to the experimental results. However, the migration paths and activation enthalpies for the +2 and +3 charge states were not calculated, and no direct comparison between all the possible charge states was made to determine which charge states dominate gallium interstitial diffusion as a function of the Fermi level. In addition, in more recent work, Schultz *et al.*²⁰ have determined that the last electron added to such density functional calculations to represent the neutral state of the tetrahedral gallium interstitial is not bound in a localized deep level, but occupies a state made out of conduction band edge states. Schultz *et al.*²⁰ conclude that any identification of favorable activation energies for neutral gallium interstitial diffusion based on calculations of the formation energy of neutral tetrahedral interstitials which assume that the last electron is bound to the interstitial in a localized deep level are not to be relied upon.

Because of the still-existing uncertainties in analyses based upon both experimental and theoretical results, a comprehensive picture of gallium interstitial diffusion, carefully considering the contributions of all possible charge states, is needed. In this paper we compute the formation energies for all the native point defects in gallium arsenide across the full range of allowed chemical potentials, from the arsenic-rich limit to the gallium-rich limit, and across the range of possible doping levels, from p -type to n -type, using an *ab initio* approach, with a single set of approximations. We compute barriers for gallium interstitial diffusion on low-energy pathways and compare our numbers to all recently available calculations for gallium interstitial formation and diffusion. We examine activation energies associated with diffu-

sion across the full ranges of chemical potential and doping. Because gallium vacancies will also contribute to diffusion of gallium, we also include in our analysis the energies associated with gallium vacancy diffusion across the full ranges of chemical potential and doping. From these energetic studies a comprehensive picture of gallium diffusion across experimentally accessible conditions emerges.

II. APPROACH

For this study we utilized codes^{28–32} implementing density-functional theory³³ within the local density approximation, with the Ceperley-Alder³⁴ form for the exchange and correlation potentials as parameterized by Perdew and Zunger.³⁵ The core electrons are treated in the frozen-core approximation and the ion cores are replaced by fully-separable³⁶ norm-conserving pseudopotentials.³⁷ Plane waves are included up to the energy cutoff of 10 Ry ($\approx 1.4 \times 10^2$ eV). The atoms are allowed to relax until the force components are less than 5×10^{-4} hartrees per bohr radius ($\approx 2.6 \times 10^{-2}$ eV/Å) and the zero temperature formation energies change by less than 5×10^{-6} hartrees ($\approx 1.4 \times 10^{-4}$ eV) per step for at least 100 steps.

For calculations of gallium interstitial migration barriers, we employed the VASP code^{29–32} with ultra-soft pseudopotentials³⁸ as supplied by G. Kresse and J. Hafner.³⁹ The nudged elastic band method^{40,41} was applied within VASP in order to determine the lowest-energy pathways for the migration of defects. All calculations were tested for consistency with the results from calculations with norm-conserving pseudopotentials. We started with the structural results of the earlier calculations and relaxed the structure with the VASP code, imposing the same convergence criteria as above, and found that the arrangements of the atoms remained unchanged. Energies computed with ultrasoft pseudopotentials were uniformly about 0.5 eV lower than those computed with norm-conserving pseudopotentials for all calculations involving a single interstitial gallium atom. The near-uniformity of this difference gives us confidence in the calculated results for the energy differences between different configurations, as well as use of the VASP code for determining the low energy migration paths and corresponding energy barriers.

The supercells we used in these calculations are based on the bulk, 216-atom cubic supercell with the bulk lattice constant determined through fitting the Murnaghan⁴² equation of state to the calculated energies as a function of the volume of the primitive cell. We found a lattice constant of 5.55 Å, which is 1.7% smaller than the experimental value of 5.65 Å at 300K and 2.2% smaller than the 1000K experimental value of 5.68 Å.⁴³ In those calculations in which we employed the VASP code we used a lattice constant of 5.59 Å determined by the same procedure. (The VASP value is 1% smaller than the 300K experimental value and 1.6% smaller than the 1000K experimental value of the lattice constant.)⁴³

In examination of the geometries of the defects, bonding characteristics, and charge distributions, we have employed the software VESTA⁴⁴ to produce the necessary volumetric plots from the results of our calculations. The volumetric plots found below also have been produced through the use of this program.

The free energy formalism¹⁰ we adopt expresses the Gibbs free energy of the system in terms of the chemical potentials of gallium ($\mu_{\text{Ga,env}}$) and arsenic ($\mu_{\text{As,env}}$) in the environment. For GaAs to be in equilibrium with its environment, these chemical potentials must be related to the chemical potential per gallium-arsenic pair in the gallium arsenide crystal as follows: $\mu_{\text{GaAs}} = \mu_{\text{Ga,env}} + \mu_{\text{As,env}}$. Furthermore, for gallium arsenide to be stable, the

magnitude of the difference between the chemical potentials of gallium and arsenic in the environment is limited to a range determined by the heat of formation of bulk gallium arsenide per atomic pair, $\mu_{\text{GaAs}} - \mu_{\text{Ga}} - \mu_{\text{As}}$, where μ_{Ga} and μ_{As} are the chemical potentials of a gallium atom in bulk gallium and an arsenic atom in bulk arsenic, respectively. For convenient calculation, the dependence of the Gibbs free energy on the chemical potential can be expressed in terms of the bulk chemical potentials and a parameter $\Delta\mu \equiv (\mu_{\text{Ga,env}} - \mu_{\text{As,env}}) - (\mu_{\text{Ga}} - \mu_{\text{As}})$. The stable range for gallium arsenide material is determined by $|\Delta\mu| \leq -(\mu_{\text{GaAs}} - \mu_{\text{Ga}} - \mu_{\text{As}})$. The resulting expression for the Gibbs free energy in this formalism¹⁰ is

$$\begin{aligned}
G_f = E(N_{\text{Ga}}, N_{\text{As}}, N_e) - TS + PV \\
- \frac{N_{\text{Ga}} + N_{\text{As}}}{2} \mu_{\text{GaAs}} \\
- \frac{N_{\text{Ga}} - N_{\text{As}}}{2} (\mu_{\text{Ga}} - \mu_{\text{As}}) - \frac{N_{\text{Ga}} - N_{\text{As}}}{2} \Delta\mu \\
- N_e \epsilon_F - N_e \Delta\Phi.
\end{aligned} \tag{1}$$

where $E(N_{\text{Ga}}, N_{\text{As}}, N_e)$ is the internal energy calculated for a given defect in a supercell consisting of N_{Ga} gallium atoms and N_{As} arsenic atoms and possessing N_e (excess) electrons which have been transferred from a reservoir with Fermi level ϵ_F . (The system is in charge state $q = -N_e$, and for defects involving a net excess of gallium or arsenic atoms, $N_{\text{Ga}} - N_{\text{As}}$ will be non-zero.)

In the gallium-rich (arsenic-rich) case, the defect is assumed to form in a sample that is in equilibrium with pure gallium (pure arsenic) with $\Delta\mu$ at its maximum (minimum) value. All the chemical potentials needed for this calculation have been computed using the same methods described above with norm-conserving pseudopotentials.

The formation entropy S consists of contributions due to the multiplicity of configurations related by symmetry operations, including different split interstitial orientations and Jahn-Teller distortions, and vibration. The vibrational entropy will be the most significant and is prohibitively expensive to calculate so it is not included in the results below. (The enthalpies of formation are used in the remaining discussions in this paper.) The PV term is unimportant in the current calculation because the energy contribution per atom (or atom pair) of this term for the materials we are discussing is on the order of 10^{-5} eV.¹⁴

Because there is no absolute alignment of eigenstates between different calculations, we calculate the electric potential along a line from the defect across the supercell and averaged over planes perpendicular to this line, according to the procedure outlined by Kohan *et al.*⁴⁵ Far from the neutral defect the plane-averaged potential converges to a fixed value. From this fixed value, we subtract the plane-averaged electric potential computed in the bulk for the same geometry to obtain the potential difference $\Delta\Phi$. This potential difference causes the energy of a defect in charge state $q = -N_e$ to be artificially shifted by $N_e \Delta\Phi$ and we compensate by subtracting this from the computed energies. (Typical values of $|\Delta\Phi|$ are around 0.05 eV.)

Previously we demonstrated¹⁴ that supercells smaller than 216 atoms do not give well-converged formation energies for isolated charged arsenic interstitials, and therefore do not produce well-converged charge transition energies for isolated arsenic interstitials in gallium arsenide. In this work we used 216-atom supercells (plus or minus defect atoms) to produce the total energies of charged and neutral defects in gallium arsenide, which are displayed in Figs. 1 and 2 for the gallium-rich and arsenic-rich limits, respectively.

The supercell approximation is known to include a non-physical interaction between the artificially-duplicated defects in different supercells. While an actual infinite-size (or even a very large-size) sample is out of the question, a suitable extrapolation may be applied to obtain a better estimate of the formation energy in the large-supercell limit. In the supercell calculation, the charge state of the defect is produced by adding or removing electrons from the defect atom and placing a homogeneous compensating charge in the background. The redistribution of charge that results when self-consistency is obtained will have a non-zero electrostatic energy of interaction between supercells, which was suggested to be properly removed by computing the dipole and quadrupole moments of the supercell and then removing the energy of the interaction between these artificially-repeated moments from the supercell result.⁴⁶ Generally, corrections of this type are more important for defect charge states farther from neutral and for smaller supercells. In the case of the gallium interstitial in the +3 state (the lowest energy state when the Fermi energy is taken at the valence band edge) we evaluated these corrections and found that they are +2.408 eV for the 65-atom supercell and -0.287 eV for the 217-atom supercell. The uncorrected energy in the larger cell is 0.3 eV higher than in the smaller cell. However adding the correction *increases* the difference between the smaller and larger supercells to around 2.4 eV in the opposite sense to the uncorrected difference. The lack of convergence in the results leads us to doubt the validity of this correction in this situation.

In a related approach to this correction, making note of the fact the original correction depends upon the bulk dielectric constant, an external parameter, some investigators fit the results using the expression $AL^{-1} + BL^{-3}$. This expression scales with supercell lattice parameter L exactly as the Makov model does, but treats the interrelated pre-factors as fitting parameters to ‘data’ constituting of formation energies computed for different L values. Corrections of this form have been employed in a variety calculations, and yet they remain controversial. Work in this area⁴⁷ has shown that this widely-applied finite scaling approach,⁴⁶ while certainly accounting for the basic effect, does not consistently produce the infinite-size limiting result. Recently a new, but related, approach has been outlined that may be used to properly remove the supercell size effect.⁴⁸ For a discussion of the situation surrounding the use of these corrections, see the review by Nieminen.⁴⁹ As a result of the continuing discussion and the uncertainty introduced by the numbers in our test calculations, we have not employed these corrections in the present results.

III. RESULTS & DISCUSSION

A. Defect energy and structure

Gallium diffusion rates can vary strongly due to varying concentrations of the gallium defects which are available to diffuse.² Gallium vacancy migration involves the motion of gallium atoms from a nearby lattice site to the vacancy site. The gallium atom moves in the opposite direction to that of the vacancy and the gallium remains on the gallium sublattice. Gallium interstitials are gallium atoms outside the crystal lattice and may move from one position to another with or without entering the gallium sublattice. Gallium antisite defects move either by the antisite atom moving into a nearby vacant site or an interstitial location. In order for gallium to move through the lattice as a gallium antisite, the antisite gallium atom must move into a nearby arsenic vacancy. However, as we will show below, arsenic vacancies are not among the most numerous defects for any equilibrium

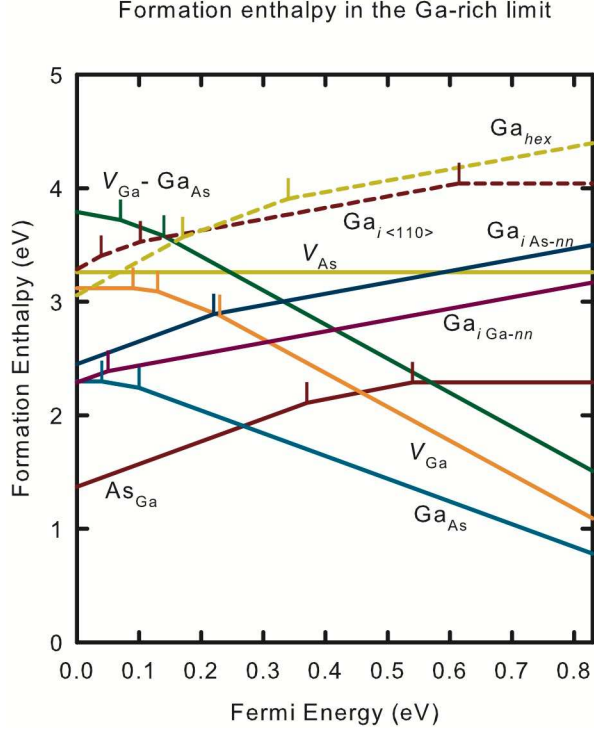


FIG. 1. (Color online) Formation energies of low-energy point defects and several gallium interstitials plotted as a function of Fermi energy across the calculated band gap in the gallium-rich limit. The meanings of the symbols are As_{Ga} = arsenic antisite, Ga_{As} = gallium antisite, V_{Ga} = gallium vacancy, V_{As} = arsenic vacancy, $\text{Ga}_{i\text{As-}nn}$ = tetrahedral gallium interstitial with arsenic nearest neighbors, $\text{Ga}_{i\text{Ga-}nn}$ = tetrahedral gallium interstitial with gallium nearest neighbors, $\text{Ga}_{i\langle 110 \rangle}$ = $\langle 110 \rangle$ gallium-gallium split interstitial, Ga_{hex} = gallium interstitial in the hexagonal position, and $V_{\text{Ga}} - \text{Ga}_{\text{As}}$ = gallium vacancy created when an arsenic vacancy is eliminated by being occupied with a neighboring gallium atom. The $V_{\text{Ga}} - \text{Ga}_{\text{As}}$ defect was first identified as the lower-energy configuration of the arsenic vacancy for Fermi energies higher in gap by Baraff and Schlüter.^{50,51} Unstable barrier configurations are indicated with dashed lines.

conditions. Therefore adding the requirement of a nearby arsenic vacancy reduces the ability for the gallium antisite to be an agent of gallium diffusion. On the other hand, if the antisite breaks apart into an independent arsenic vacancy and an independent gallium interstitial, then gallium diffusion would proceed via an interstitial pathway as described above. So we focus on the basic processes of gallium interstitial diffusion in our calculations and consider only the competition between gallium interstitial diffusion and gallium vacancy diffusion in our final analysis of gallium diffusion.

Relative concentrations of gallium and arsenic in the environment when gallium arsenide is grown will affect the concentrations of defects containing an excess of gallium or arsenic which are present in the material after growth. In other words, the equilibrium concentrations of defects involving an excess of one of the native species or the other will be controlled by the chemical potential. Gallium arsenide material is stable when the chemical potential falls within the allowed compositional range, between the arsenic-rich and gallium-rich limits. The Fermi energy will also affect the equilibrium concentrations of most defects because they can exist in many different charged states, which can be formed by donating or accept-

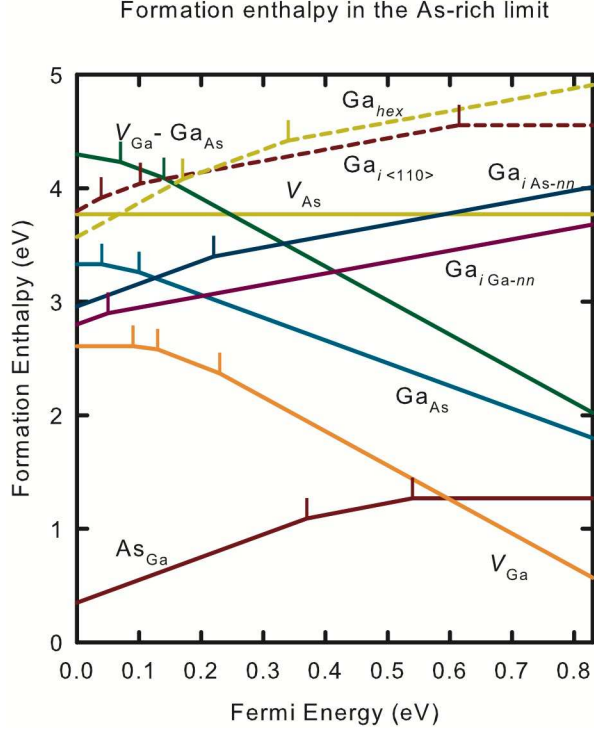


FIG. 2. (Color online) Formation energies of low-energy point defects and several gallium interstitials plotted as a function of Fermi energy across the calculated band gap in the arsenic-rich limit.

ing electrons from the crystal. Under equilibrium conditions we can estimate the expected concentrations of each of these defects from their formation energies.

We present enthalpies of formation for the complete set of point defects which may play a role in gallium diffusion, according to our calculations, as a function of Fermi energy in Figs. 1 and 2, in the gallium-rich and arsenic-rich limits, respectively. In order to determine which defect configurations and charge states are likely to play an important role in gallium diffusion, we relaxed numerous initial defect configurations into their lowest-energy geometries, using the approach and convergence limits described in Section II.⁵² We have included in Figs. 1 and 2 various configurations of gallium interstitials as well as gallium and arsenic vacancies and gallium and arsenic antisites, but we have not included arsenic interstitials, since they are not expected to play a direct role in gallium diffusion, and arsenic interstitial formation energies are large enough so that charged arsenic interstitial concentrations are too low to change the effective doping significantly enough to affect the concentrations of other charged defects over the entire range of conditions considered in Section III B, from *p*-type to *n*-type and from Ga-rich to As-rich.

The dependence of the formation energy for each defect upon the chemical potential can be seen by comparing the energies of formation in Figs. 1 and 2 for the same defect to each other. Defects with excess gallium possess lower energies in Fig. 1, which represents the gallium-rich limit, and higher energies in Fig. 2. The opposite is the case for defects with an excess of arsenic.

The formation energy of each specific defect in Figs. 1 and 2 is presented as a continuous graph of a set of straight segments representing the energy to form the lowest-energy charge

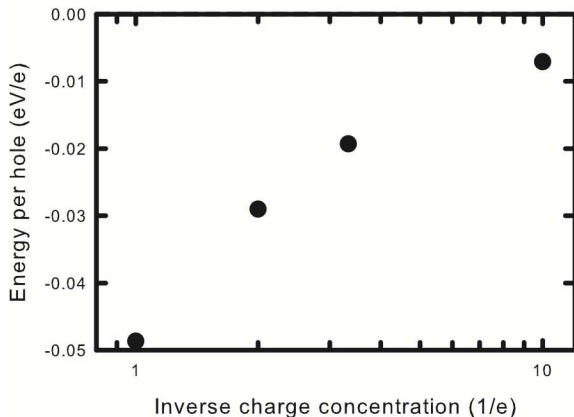


FIG. 3. The energy per hole for the transition between the neutral 216 atom GaAs supercell and an equivalent supercell in a positive charge state q is displayed as a function of the reciprocal of the charge state. The origin of the energy axis is placed at the valence band edge, defined as the energy of the highest occupied Kohn-Sham state.

state of the specified defect. The slope of each segment corresponds to the charge of the lowest-energy state of the defect in units of the fundamental charge e . The Fermi energies corresponding to the points at which two of the straight segments in the graph are joined are the charge transition levels. The charge transition levels are indicated with vertical lines in these figures.

The Fermi energy in Figs. 1 and 2 covers the range from 0 eV to 0.83 eV, corresponding to the energy range from the highest occupied to the the lowest unoccupied Kohn-Sham state (at the Γ point) in the bulk calculation. Lany and Zunger⁵³ have justified the identification of this energy range as the calculated band gap by showing that valence band edge defined as the difference in energy between the neutral and the +1 state for the bulk semiconductor in the dilute limit, corresponding to adding one hole to an infinitely large bulk crystal, and the conduction band edge defined as the difference in energy between the -1 and the neutral state for the bulk semiconductor in the dilute limit, corresponding to adding one conduction electron to an infinitely large bulk crystal, are equal to the energies of the highest occupied and lowest unoccupied Kohn-Sham states at the Γ point in the bulk calculation, respectively, in the direct-gap semiconductor ZnO. We have verified that the difference in energy between the neutral and the +1 state for the bulk semiconductor approaches the Kohn-Sham energy of the highest occupied state in the dilute limit and the difference in energy between the -1 and the neutral state for the bulk semiconductor approaches the Kohn-Sham energy of the lowest unoccupied state in the dilute limit in our calculations as well. The results of this calculation for the valence band edge are shown in Fig. 3.

At the current time, there is ongoing discussion about the underestimation of the band gap in standard density functional calculations and the effect of this on comparing density functional results for defect properties to experimental results,^{20,54–56} including whether and when a shift of transition levels by the so-called ‘scissors operator’^{57,58} is justified. A full evaluation of every possible approach to correcting this problem is beyond the focus of this paper. Instead, we present the formation energies as they are calculated and describe the character of the associated electronic states for those cases in which there may be a

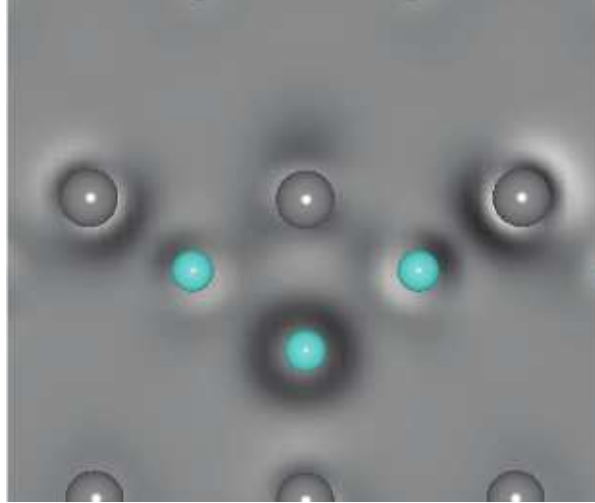


FIG. 4. (Color online) The difference in the distribution of electrons, when the tetrahedral gallium defect charge state is changed from doubly positive to singly positive, is displayed in this gray scale image. The interstitial is shown in a (110) plane containing one of the bonding chains of gallium and arsenic just above the interstitial. The darker regions indicate an increase in the electron density due to the transition from the more positive charge state to the less positive charge state. The lighter regions indicate a depletion of electron density due to the same transition. The very dark region surrounding the interstitial atom indicates a substantial increase in electron density in this region due to the added electron.

special need to make corrections. When performing the analysis for diffusion, we employ the as-calculated numbers and also make reasonable estimates for the effects of corrections for the few cases in which such corrections may be needed. We obtain clear predictions for diffusion from this set of calculations, which are in reasonable agreement with all other recent calculations of one or another of the quantities reported here.

Gallium interstitials are found to favor tetrahedral interstitial positions in our own calculations, as in the results of Malouin *et al.*²¹ and Schultz *et al.*²⁰ In our results, the gallium in the tetrahedral interstitial position surrounded by gallium atoms possesses the lowest formation enthalpy for charge states from neutral through doubly positive for all interstitial configurations. In the triply positive charge state, the tetrahedral positions between either gallium or arsenic atoms have nearly the same energy cost. Comparison of our formation energies to those of Schultz *et al.*, who finds that the tetrahedral gallium interstitial surrounded by arsenic atoms is the favorable configuration for the non-zero charge states,²⁰ shows differences of up to about 0.2 eV, an amount comparable to the uncertainty of our density functional results, for all the point defects we can compare.

The outer three electrons of the neutral gallium atom, which are involved in the bonding in GaAs, occupy 3s (two electrons) and 3p (the third electron) states in the case of an isolated gallium atom. When this atom occupies a tetrahedral interstitial position in GaAs, it is far enough from the bonding chains that the two electrons filling the 3s states, which lie closer to the gallium nucleus, may not be greatly perturbed by the surrounding lattice, while the last electron, which must occupy a higher energy state, may be strongly affected.

In order to examine the spatial distribution of the states occupied by these three outer electrons for a tetrahedral gallium interstitial in GaAs, we show the redistribution of charge

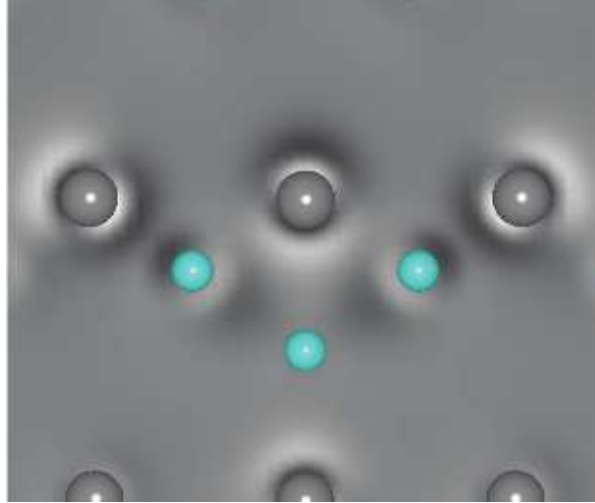


FIG. 5. (Color online) The difference in the distribution of electrons, when the tetrahedral gallium defect charge state is changed from singly positive to neutral, is displayed in this gray scale image. Here we see no large increase in the electron density in the immediate neighborhood of the interstitial due to the added electron. Instead, the added electron density is spread out across a wide region of the surrounding bonding chains.

as the tetrahedral gallium interstitial between gallium atoms makes charge state transitions from doubly positive to singly positive and from singly positive to neutral, respectively, in Figs. 4 and 5. The dark regions in the figure represent regions in which negative charge is added in each transition to the less positive charge state. We have also examined the redistribution for the transition from triply positive to doubly positive and found that this produced an image similar to Fig. 4, which we do not present here because of this similarity.

To understand these images it is easiest to begin with the triply positive state, which is a gallium nucleus and its core electrons occupying the tetrahedral interstitial position between gallium atoms. The charge density changes for each transition provide a map of the spatial distribution of the state occupied by the added electron. The first two electrons added, which make the transitions from triply positive to doubly positive and then from doubly positive to singly positive, can be seen to occupy s -orbital-like states, strongly concentrated in a spherically symmetric region close to the tetrahedral gallium atom. The image in Fig. 4 shows the electron going into a tight, spherically symmetric region around the tetrahedral gallium atom, and not forming bonds with neighboring atoms. We conclude that the associated transition levels correspond to strongly localized, low-energy s -like deep levels, and are correctly positioned with respect to the valence band edge.

In order to examine the spatial distribution of the state occupied by the last of the three outer electrons, we show the redistribution of charge as the tetrahedral gallium interstitial between gallium atoms makes the transition from singly positive to neutral in Fig. 5. We can see that this last electron occupies a wide region surrounding the defect, involving the neighboring atoms for some distance. We conclude that any strongly localized, $3p$ -derived state for this last electron must be at a higher energy than the conduction band edge states in this calculation, and that the calculated transition level between the singly positive and neutral charge states for this interstitial, which is very near the calculated conduction band edge, actually corresponds to putting the final electron into conduction band edge

states rather than into a localized deep level on the interstitial. This result is in agreement with the analysis presented in Ref. 20, which also concludes that the localized deep level corresponding to the neutral tetrahedral gallium interstitial between gallium atoms must be a resonance in the conduction band.

An electron at the conduction band edge in the vicinity of a singly positive tetrahedral interstitial can lower its energy by occupying a shallow hydrogenic bound state composed of conduction band edge states, so that there will be a transition to the neutral interstitial charge state just below the conduction band edge, with the final electron occupying such a shallow hydrogenic bound state. Our estimates for such a state using the experimental static dielectric constant of 12.85 for GaAs⁴³ give a binding energy of about 5.5 meV with an effective Bohr radius of around 100 Å, which is much larger than the dimension of the supercell used in our calculations. Since our density functional calculations put the last electron in the lowest energy state, this electron should be observed to occupy the shallow hydrogenic bound state. However, due to size restrictions, the density functional calculation cannot properly represent the spatial distribution of this state.

Because the calculated energies of both the conduction band edge states and the hydrogenic bound state composed of these states are lower than they should be as a result of the known issues of density functional theory in the local density approximation, the formation energy of the neutral tetrahedral gallium interstitial between gallium atoms will be underestimated. The calculated formation energy for the neutral tetrahedral gallium interstitial between gallium atoms (with the last electron occupying a shallow hydrogenic bound state composed of conduction band states) should be shifted up by a scissors-type correction — as is done for the conduction band edge states, to shift the calculated conduction band edge up to match the experimental gap — in order to correctly represent a transition level just below the conduction band edge for the transition from singly positive to neutral, with the last electron occupying the shallow hydrogenic bound state.

In order to calculate the scissors correction which must be applied to the formation energy of the neutral tetrahedral interstitial surrounded by gallium atoms, it is necessary to take into account the fact that the Γ point is not included in the Monkhorst-Pack mesh⁵⁹ we use for the summation over k -points in our defect calculations. Therefore the energy of the lowest available conduction band states, out of which the hydrogenic bound state of the defect is formed, is higher than the calculated conduction band edge at the gamma point by 0.356 eV. We determined this difference between the effective conduction band edge in our defect calculations and the calculated band edge at the Γ point by taking the difference between the energy of the lowest conduction band states in the bulk calculation including the same k -points that we included in our defect calculations and the energy of the conduction band edge at the Γ point from a bulk calculation. The calculated +1/0 transition level for the neutral tetrahedral interstitial surrounded by gallium atoms is just below the effective conduction band edge for our defect calculations, at 0.330 eV above the calculated band edge at the Γ point. Our calculations therefore give a binding energy of 26 meV for the electron bound to the neutral tetrahedral interstitial in the shallow hydrogenic bound state. We do not expect our calculations to give a binding energy which matches the estimated binding energy of 5.5 meV for an electron bound to an isolated positively charged defect in a shallow hydrogenic state with an effective Bohr radius of around 100 Å, since the supercell dimensions in our defect calculations are much smaller than 100 Å, forcing the bound electron to be much closer than 100 Å to the nearest defect in the periodic array of defects in our supercells.

The scissors correction for the formation energy of the neutral tetrahedral interstitial surrounded by gallium atoms should be large enough to raise the +1/0 transition level from just below the calculated effective conduction band edge in our defect calculations to just below the experimental conduction band edge. Since the experimental band gap depends on temperature, the scissors correction will also depend on temperature. In our calculations of activation energies for diffusion, we will shift the formation energy of any neutral defect with its last electron occupying a hydrogenic bound state composed of the lowest available conduction band states up by the same scissors correction as is needed to shift the effective conduction band edge in our defect calculations up to coincide with the experimental conduction band edge. Further corrections to remove the errors in the calculated binding energy of the hydrogenic state which occur due to the size of the supercells are not made, since they are within the estimated uncertainty of these calculations due to other causes.

As we have argued above, the existence of a shallow hydrogenic bound state for the gallium tetrahedral interstitial between gallium atoms means that there must be a transition level between the singly positive state and the neutral state just below the conduction band edge. We also find a transition level between the triply- and doubly-positive charge states essentially at the valence band edge. We conclude that the lowest energy interstitial defect for an excess gallium atom in gallium arsenide is the tetrahedral interstitial with four gallium nearest neighbors in the neutral, singly-, doubly-, and triply-positive charge states, depending on Fermi energy, across the calculated band gap. As the Fermi energy approaches the valence band edge, the triply-positive and doubly-positive charge states become very nearly equally energetically favorable. We also note that the formation energy for the tetrahedral gallium interstitial surrounded by arsenic atoms in the triply-positive charge state is nearly the same as that for the tetrahedral gallium interstitial surrounded by gallium atoms in this charge state.

Just as the effective conduction band edge in our defect calculations is higher than the calculated conduction band edge at the Γ point, the effective valence band edge in our defect calculations is lower than the calculated valence band edge at the Γ point, due to the fact that the Monkhorst-Pack mesh we use does not include the Γ point. This helps to ensure that when the last two electrons are removed from the tetrahedral interstitial surrounded by gallium atoms, in order for this interstitial to make the transitions to the +2 and +3 charge states, these electrons are removed from highly localized defect states rather than delocalized valence band states. We can also see that these last two electrons are removed from localized defect states, producing defects which are truly in the +2 and +3 charge states, by reviewing Fig. 4, which shows the redistribution in charge resulting from the +2/+1 transition, and which looks essentially the same as a similar figure showing the redistribution in charge resulting from the +3/+2 transition. We have not shown the figure for the +3/+2 transition due to this similarity. Although the +3 charge state is not the charge state with the highest concentration for any Fermi level in the gap (since the +3/+2 transition for the gallium tetrahedral interstitial between gallium atoms occurs essentially at the valence band edge), we note that this charge state may still dominate diffusion if the migration barriers for diffusion in the +3 charge state are low enough that the total activation energy for diffusion (formation energy plus migration barrier) is lowest for these charge states. For this reason, we consider diffusion in all charge states from +3 to neutral for the low-energy diffusion paths considered in this paper.

When we examine the properties of the tetrahedral gallium interstitial surrounded by

arsenic atoms, we find that they are quite similar to the properties of the slightly more energetically favorable tetrahedral gallium interstitial surrounded by gallium atoms. In particular, we find that the redistribution of charge as the tetrahedral interstitial between arsenic atoms makes a transition from the doubly positive to the singly positive charge state is similar to the redistribution of charge as the tetrahedral interstitial between gallium atoms makes this charge state transition, as shown in Fig. 4 and discussed above. This shows that the electron which is added in order to accomplish this charge transition goes into a highly localized state in the vicinity of the defect for both tetrahedral interstitials. We also find that the redistribution of charge as the tetrahedral interstitial between arsenic atoms makes a transition from the singly positive to the neutral charge state is similar to the redistribution of charge as the tetrahedral interstitial between gallium atoms makes this charge state transition, as shown in Fig. 5 and discussed above. This shows that the last electron which is added in order to accomplish the transition to the neutral charge state goes into a delocalized conduction-band-like state for both tetrahedral interstitials. We conclude that the last electron goes into delocalized states at the conduction band edge in the supercell calculations for both of the neutral tetrahedral gallium interstitials, in agreement with Schultz *et al.*²⁰.

As we have discussed above, in the vicinity of a defect in the +1 charge state, an electron at the conduction band edge can lower its energy by occupying a shallow hydrogenic bound state composed of conduction band edge states. We conclude that there will be a transition to the neutral interstitial charge state just below the conduction band edge, with the final electron occupying such a shallow hydrogenic bound state, for the tetrahedral interstitial surrounded by arsenic atoms, as there is for the tetrahedral interstitial surrounded by gallium atoms. As discussed above, the calculated formation energy for any neutral defect with its last electron occupying a shallow hydrogenic bound state composed of conduction band states should be shifted up by a scissors-type correction — as is done for the conduction band edge states, to shift the calculated conduction band edge up to match the experimental gap — in order to correctly represent a transition level just below the conduction band edge for the transition from singly positive to neutral. As we do for the neutral tetrahedral interstitial surrounded by gallium atoms, in our calculations of activation energies for diffusion, we will shift the formation energy of the neutral tetrahedral interstitial surrounded by arsenic atoms up by the same scissors correction as is needed to shift the effective conduction band edge in our defect calculations up to coincide with the experimental conduction band edge.

We find that the gallium hexagonal interstitial configuration is unstable in all charge states across the band gap, and will relax to lower energy configurations if allowed, as first shown by Malouin *et al.*²¹ By investigating the changes in the distribution of charge when the hexagonal gallium interstitial charge state is changed from singly positive to neutral, we find that the electron which is added to complete this transition occupies a delocalized conduction-band-like state, as was the case for the neutral tetrahedral interstitial surrounded by gallium atoms, discussed above. As in the earlier case, an electron at the conduction band edge in the vicinity of a singly positive hexagonal interstitial can lower its energy by occupying a shallow hydrogenic bound state composed of conduction band edge states, so that there will be a transition to the neutral interstitial charge state just below the conduction band edge, with the final electron occupying a shallow hydrogenic bound state. The calculated +1/0 transition level for the neutral hexagonal interstitial is just below the effective conduction band edge for our defect calculations, at 0.326 eV above the calculated band edge at the Γ point, which gives a binding energy of 30 meV for the electron bound

to the neutral hexagonal interstitial. As in the case of the neutral tetrahedral interstitials, in our calculations of activation energies for diffusion, we will shift the formation energy of the neutral hexagonal interstitial up by the same scissors correction as is needed to shift the effective conduction band edge in our defect calculations up to coincide with the experimental conduction band edge.

We find that the gallium bond-centered interstitial configuration is also unstable in all charge states across the band gap, and will relax to lower energy configurations if allowed, as first shown by Malouin *et al.*²¹. When we relaxed the bond-centered interstitial, we discovered that it generally relaxes in the direction of the tetrahedral interstitial, a view also supported by the work of Malouin *et al.*²¹ In a slightly different result, Schultz *et al.*²⁰ found that the bond-centered gallium interstitial relaxes to two configurations of lower symmetry which have been designated as gallium-arsenic split interstitials by Malouin *et al.*²¹ In one of our calculations, we also observed a neutral bond-centered interstitial relaxing into a gallium-arsenic split interstitial, in which the excess gallium atom shares an arsenic lattice site with an arsenic atom. From these results, one may conclude that these split interstitial configurations are lower in energy than the original bond-centered configuration.

A gallium split interstitial geometry involves an excess gallium atom sharing a lattice site with the atom associated with that lattice site. The arrangement of the split interstitial atoms may be symmetric with respect to exchange of the atoms if they are of the same type, but the center of mass of the pair of atoms is typically moved away from the lattice location. Different gallium split interstitial configurations on same lattice site, having different orientations of the axis of the split interstitial pair and therefore different bonding with the atoms on the neighboring lattice sites, may have quite different energies.

Metastable gallium split interstitial configurations which have been found in previous work^{20,21} include gallium-arsenic $\langle 110 \rangle$ and $\langle 111 \rangle$ split interstitials (using the nomenclature of Malouin *et al.*²¹), where the gallium atom shares an arsenic lattice site with the arsenic atom originally associated with that site, and gallium-gallium $\langle 110 \rangle$ and $\langle 100 \rangle$ split interstitials, where the gallium atom shares a gallium lattice site with the gallium atom originally associated with that site. The same split interstitial configuration is not always found to be metastable in all the same charge states in References 21 and 20. For example, the gallium-gallium $\langle 110 \rangle$ split interstitial is not identified as a metastable configuration for any charge state and is therefore not studied by Malouin *et al.*²¹.

However, both of these earlier papers (and our work) agree on the general ordering of these split interstitial configurations, where they have been calculated. For example, the gallium-gallium $\langle 100 \rangle$ split interstitial has been found to be the highest in energy (or at least tied for the highest) in the neutral and positive charge states.^{20,21} Both Malouin *et al.*²¹ and Schultz *et al.*²⁰ identify the configuration called a $\langle 111 \rangle$ gallium-arsenic split interstitial by Malouin *et al.*²¹ as the lowest energy non-tetrahedral configuration for the +1 charge state, with a formation energy 0.93 eV above the formation energy of the most energetically favorable tetrahedral interstitial according to Malouin *et al.*,²¹ and 0.95(0.83)eV above the formation energy of the most energetically favorable tetrahedral interstitial according to the LDA(PBE) calculations of Schultz *et al.*²⁰ For the +2 and +3 charge states, Malouin *et al.*²¹ identify the $\langle 111 \rangle$ gallium-arsenic split interstitial as the lowest energy non-tetrahedral configuration, at 0.93 eV above the formation energy of the most energetically favorable tetrahedral interstitial (for both charge states), but they have no calculations for the gallium-gallium $\langle 110 \rangle$ split interstitial. Schultz *et al.*²⁰ identify the gallium-gallium $\langle 110 \rangle$ split interstitial as the lowest energy non-tetrahedral configuration for the +2 and +3 charge states, at 0.9-1.0 eV higher

than the formation energy of the tetrahedral interstitial surrounded by arsenic atoms, but they do not report any calculations for gallium-arsenic interstitials in these charge states, since they do not find the gallium-arsenic split interstitial configurations to be metastable for these charge states.

Although Malouin *et al.*²¹ do not consider the gallium-gallium $\langle 110 \rangle$ split interstitial configuration, both Schultz *et al.*²⁰ and our present work find this configuration to be the lowest energy metastable non-tetrahedral configuration for the neutral charge state. We find the formation energy of the neutral $\langle 110 \rangle$ split interstitial to be only 0.53(0.57) eV above the formation energy of the most energetically favorable tetrahedral interstitial, according to our norm-conserving pseudopotential (VASP) calculations. Schultz *et al.* report the formation energy of the neutral $\langle 110 \rangle$ split interstitial to be 0.6-0.7 eV above the formation energy of the most energetically favorable tetrahedral interstitial.²⁰ The next higher energy configuration found for the neutral gallium interstitial is the $\langle 111 \rangle$ gallium-arsenic split interstitial, with a formation energy reported at 0.82 eV above the formation energy of the most energetically favorable tetrahedral interstitial by Malouin *et al.*,²¹ and 0.9 eV above the formation energy of the most energetically favorable tetrahedral interstitial by Schultz *et al.*²⁰

We note that for all non-neutral charge states that seem likely to play an important role in gallium interstitial diffusion ($q = +1, +2, \text{ and } +3$), the formation energy of the lowest energy metastable non-tetrahedral configuration found by us or in previous work^{20,21} is 0.8-0.9 eV above the energy of the most energetically favorable tetrahedral interstitial. We conclude that the energy barrier for neutral gallium interstitial diffusion via a path going through the gallium-gallium $\langle 110 \rangle$ split configuration may be lower than the energy barrier for any other charge state and diffusion pathway. We will therefore investigate the $\langle 110 \rangle$ split interstitial more closely.

The neutral tetrahedral gallium interstitial surrounded by gallium atoms and the neutral gallium-gallium $\langle 110 \rangle$ split interstitial configurations are compared in Fig. 6. The neutral gallium interstitial with gallium nearest neighbors is shown in Fig. 6(a), where the interstitial is seen as an isolated atom to the left of the center, surrounded by four gallium atoms. Additional atoms from the lattice are shown around the defect to enable ease of comparison to the $\langle 110 \rangle$ split interstitial that is shown in Fig. 6(b).

As can be seen in Fig. 6(a), tetrahedral gallium interstitials maintain the symmetry of the ideal tetrahedral defect, with an outward relaxation of the neighboring atoms. There is an outward relaxation of the four nearest neighbor gallium atoms by about 6.3%, to a distance of 2.55 Å from the neutral tetrahedral gallium interstitial. (This may be compared to the 2.48 Å distance between the nearest-neighbor atoms in bulk gallium.) The bulk nearest neighbor distance in GaAs is 2.40 Å, as determined with the same code and within the same standards of convergence described previously. The distances between the pairs of nearest-neighbor lattice gallium atoms around the defect is 4.17 Å, where the corresponding bulk next-nearest neighbor distance is 3.96 Å, *i.e.* there is a 5.3% expansion.

For the neutral tetrahedral gallium interstitial with arsenic nearest neighbors, the As neighbor atoms relax by about 5.4% outward to a distance of 2.53 Å. The spacing between the four nearest-neighbor As atoms surrounding the interstitial in this case is 4.14 Å, an expansion of 4.5%.

A picture of the bonding in the neighborhood of a defect can be obtained by plotting the electron localization function,⁶⁰ which is shown in Fig. 7 for the neutral tetrahedral interstitial with gallium nearest neighbors. As can be seen in Fig. 7, the interstitial gallium atom is not bonded to the four nearest neighbor gallium atoms. This is consistent with

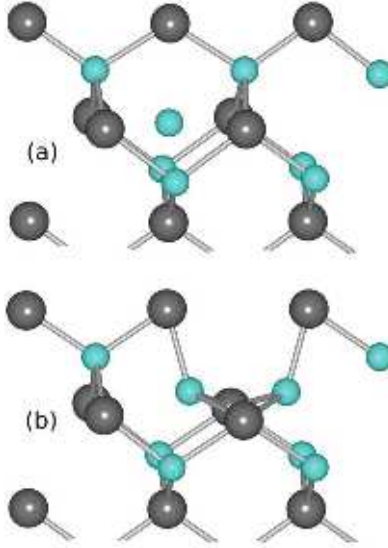


FIG. 6. (Color online) Comparison of neutral gallium interstitials in the tetrahedral position between gallium atoms (a) and in the gallium-gallium $\langle 110 \rangle$ split configuration (b). The split interstitial is metastable in this charge state. Gallium atoms are represented with smaller light blue spheres and the arsenic atoms with larger dark gray spheres. A small number of the lattice atoms surrounding the interstitial are presented in these figures for the sake of clarity.

a picture in which the highest occupied state is a hydrogenic level that is spread over the volume of the supercell. We can also see a high amount of electron localization in a small, spherically symmetric region surrounding the interstitial atom, indicating that the other two valence electrons which are bound to this neutral interstitial are in highly localized, spherically symmetric, s -like states.

The metastable neutral gallium-gallium $\langle 110 \rangle$ split interstitial configuration is shown in Fig. 6(b). The center of the gallium split-interstitial pair is 0.85 \AA below the ideal gallium lattice site, as shown in Fig. 6(b). The distance between the two gallium atoms of this split interstitial is 2.74 \AA , which is 15% farther than the calculated bulk gallium arsenide nearest neighbor distance of 2.40 \AA . Either arsenic atom shown bonding to, and above, the split interstitial in Fig. 6(b) is 2.46 \AA from the nearest gallium atom of the split pair, and the two arsenic atoms shown bonding to, and below, the defect are 2.58 \AA from either gallium in the defect. Each split-interstitial gallium atom is 2.83 \AA from the nearest other gallium atom in the crystal. We note that the gallium-gallium $\langle 110 \rangle$ split interstitial is closer to the original gallium lattice site, and the distance between the two atoms of the gallium split-pair is larger than the corresponding distances¹⁴ in the arsenic-arsenic $\langle 110 \rangle$ split interstitial.

We may also compare the distance between the two gallium atoms of the split interstitial to interatomic distances in the room-temperature phase (α -gallium) of pure gallium. In α -gallium, the atoms have one nearest neighbor at 2.39 \AA and four next-nearest neighbors at distances ranging from 2.71 \AA to 2.80 \AA .⁶¹ We find that the gallium split-pair atoms are separated from each other by a distance within the range of the next-nearest neighbors in bulk gallium.

The lattice is expanded slightly and neighboring atoms move outward around a split interstitial, as they do around a tetrahedral interstitial. The distance between the two

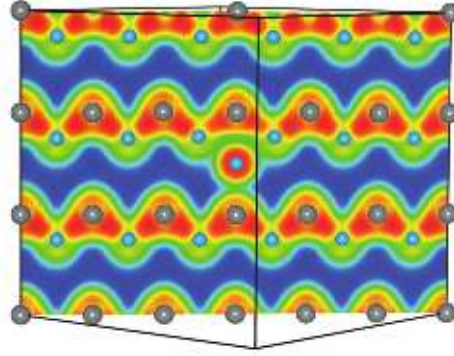


FIG. 7. (Color online) The electron localization function⁶⁰ in a supercell containing a neutral gallium tetrahedral interstitial surrounded by gallium nearest neighbors is displayed for a (110) plane passing through the interstitial atom. Gallium atoms are represented with smaller blue spheres and arsenic atoms, with larger gray spheres. Atoms between the plane and the viewer have been removed for the sake of clarity. Higher values of the electron localization function are shown in red. The color yellow corresponds to the value of 0.5, below which the localization function is too weak to indicate bonding. The interstitial is seen between two parallel bonding chains near the center of the figure. Two of the nearest-neighbor gallium atoms are visible immediately above the defect, just to the left and right. The remaining two nearest neighbor gallium atoms are associated with a chain perpendicular to the plane shown here, and belong to a bonding chain that includes the arsenic atom immediately below the interstitial. There is little evidence of bonding between the tetrahedral interstitial and any of the nearby atoms.

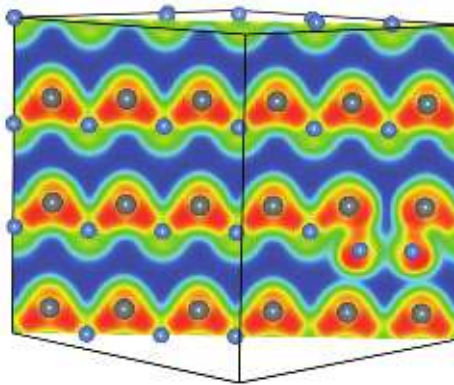


FIG. 8. (Color online) The electron localization function⁶⁰ in a supercell containing a neutral $\langle 110 \rangle$ Ga-Ga split interstitial is displayed for a (110) plane passing through the interstitial atom. Gallium atoms are represented with smaller blue spheres and arsenic atoms, with larger gray spheres. Atoms between the plane and the viewer have been removed for the sake of clarity. Higher values of the electron localization function are shown in red. The color yellow corresponds to the value of 0.5, below which the localization function is too weak to indicate bonding. The defect is located in the lower right quadrant of the figure where two gallium atoms are seen to be displaced downward from the middle chain of bonds. The two gallium atoms of the split interstitial are displaced symmetrically from a gallium lattice site on this bonding chain. The results show that the two gallium atoms of the split interstitial are not bonded to each other, while each of these gallium atoms is strongly bonded to the nearest arsenic atom along the chain.

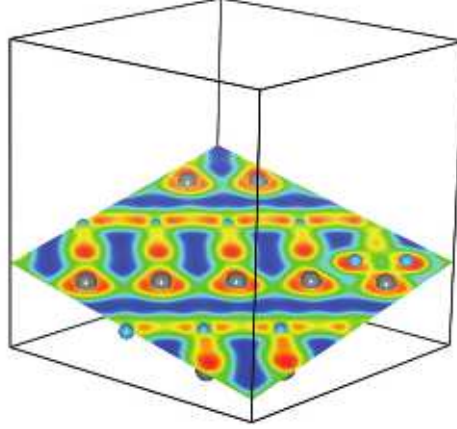


FIG. 9. (Color online) The electron localization function⁶⁰ in a supercell containing a neutral $\langle 110 \rangle$ Ga-Ga split interstitial is displayed for a (110) plane that passes through the two gallium atoms of the interstitial as well as one of the two nearest-neighbor arsenic atoms in the bonding chain perpendicular to the axis of the split interstitial. For clarity, only atoms very near this plane are shown. Some bonding is visible between each of the two gallium atoms of the defect and the nearest neighbor arsenic atom of the perpendicular chain.

arsenic atoms above the split interstitial in Fig. 6(b) is 4.02 \AA . The distance between the two arsenic atoms shown below the split interstitial in Fig. 6(b) is 4.18 \AA . The distance between any one of the arsenic atoms below the split interstitial in the figure and either one of the two arsenic atoms above the interstitial is 4.15 \AA . (For comparison, the calculated bulk gallium arsenide next-nearest neighbor distance is 3.92 \AA .)

As we can see in Fig. 6, the extra gallium atom does not have to move far for the tetrahedral interstitial between gallium atoms to transform into a gallium-gallium $\langle 110 \rangle$ split interstitial. In moving from the tetrahedral interstitial location to become part of the split interstitial defect, the Ga atom is displaced a total of 0.81 \AA .

The bonding between the two gallium atoms of the neutral $\langle 110 \rangle$ split interstitial, and between these atoms and their arsenic nearest neighbors, is investigated in Fig. 8 and Fig. 9. The electron localization function is shown for a plane cutting through the split interstitial and the $\langle 110 \rangle$ chain parallel to the axis of the split interstitial in Fig. 8. This figure shows that the two gallium atoms of the interstitial are strongly bonded to the nearest arsenic atoms in this chain, but they are not bonded to each other. The visible lack of bonding between the two gallium atoms of the split interstitial in this figure is not very surprising, since we have mentioned above that the distance between these two atoms is larger than the nearest-neighbor distance in GaAs, the distance between the two arsenic atoms of the equivalent arsenic-arsenic $\langle 110 \rangle$ split interstitial in GaAs, and the nearest neighbor distance in the room-temperature phase of bulk gallium.

In addition to the strong bonding between the gallium atoms of the split interstitial and their arsenic nearest neighbors on the $\langle 110 \rangle$ chain parallel to the interstitial axis, shown in Fig. 8, there is some weaker bonding between both gallium atoms of the split interstitial and the other two arsenic nearest neighbors of the interstitial lattice site, which are on the bonding chain perpendicular to the axis of the split interstitial. This bonding is visible in Fig. 9, which shows the electron localization function in the plane that cuts through the split interstitial and one of these arsenic atoms (the next arsenic atom closer to the viewer).

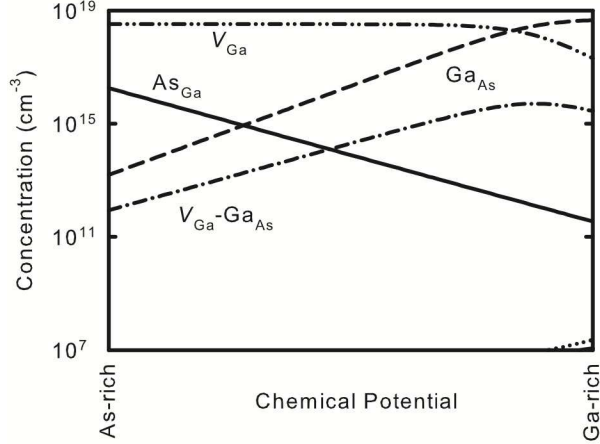


FIG. 10. Calculated equilibrium concentrations of the most common point defects at 1100 K in n -type gallium arsenide with a net donor concentration $N_d = 10^{19} \text{ cm}^{-3}$, as a function of chemical potential across the stoichiometric range.

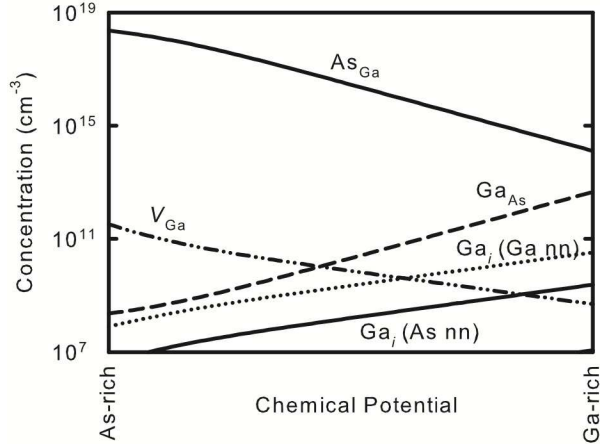


FIG. 11. Calculated equilibrium concentrations of the most common point defects at 1100 K in p -type gallium arsenide with a net donor concentration $N_d = -10^{19} \text{ cm}^{-3}$, as a function of chemical potential across the stoichiometric range.

B. Equilibrium defect concentrations

The concentrations of defects in the material under conditions of thermal equilibrium at a given temperature are determined by a self-consistent procedure in which a full account is taken of the effective doping concentration, chemical potential, and overall charge neutrality. When the chemical potential is within the range in which gallium arsenide can form, then the majority of the atoms fall into the usual lattice for that material. The concentration of a particular defect in a specific charge state is proportional to a Boltzmann factor,

$$N_s e^{-G_{f,i}(N_{\text{Ga}}, N_{\text{As}}, N_e)/kT}, \quad (2)$$

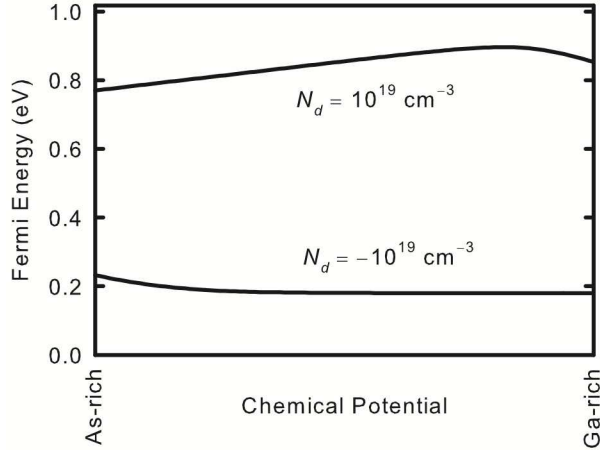


FIG. 12. Fermi energies in p - and n -type gallium arsenide as a function of chemical potential across the stoichiometric range. The full experimental band gap at 1100 K extrapolated from experiment is presented on the vertical axis.⁴³ The lower energy curve is the Fermi energy for the p -type material and the higher energy curve is the Fermi energy for the n -type material, as indicated by the doping levels N_d . Both are calculated at a temperature of 1100 K.

where $G_{f,i}(N_{\text{Ga}}, N_{\text{As}}, N_e)$ is the formation energy for defect i in charge state $q = -N_e$ calculated from Eq. 1, the net excess (or deficit) of Ga atoms involved in the defect is given by $N_{\text{Ga}} - N_{\text{As}}$, and N_s is the concentration of sites available for this defect. (Please note that the specification of the defect also includes its configuration: *e.g.* a gallium interstitial in a tetrahedral site with gallium nearest neighbors.) This formation energy depends explicitly on the chemical potential and Fermi energy.

We determine the concentrations of all the defects by requiring charge neutrality as given in the following equation:

$$N_d = \sum_{i, N_e} N_e N_s e^{-G_{f,i}(N_{\text{Ga}}, N_{\text{As}}, N_e)/kT} - N_v e^{-\epsilon_F/kT} + N_c e^{-(E_g - \epsilon_F)/kT}, \quad (3)$$

where the effective doping concentration, N_d , is given by the concentration of ionized donor impurities minus the concentration of ionized acceptor impurities.^{10,14} The second and third terms on the right hand side of Eq. 3 correspond to subtracting the density of holes in the valence band and adding the density of electrons in the conduction band, respectively, with N_v and N_c determined from experiment as described in Ref. 43.

At each temperature, this calculation is performed for values of the chemical potential over the entire compositional range from arsenic rich to gallium rich, giving the value of the Fermi energy and the resulting concentrations of all the charged defects, which depend on the Fermi energy. In doing this calculation, the band-gap in gallium arsenide is taken to be the experimentally determined gap or the gap extrapolated from experiment,⁴³ and the defect formation energies are those produced by the present density-functional calculation. Scissors corrections for charge state transition levels involving movement of an electron to or from a localized state with conduction-band-like character, such as the donor levels of the arsenic antisite, do not make a qualitative difference in Figs. 10 to 12; they do not change the ordering of the most numerous defects.

Our estimated equilibrium concentrations are displayed for an annealing temperature of 1100 K for both strong n -type and strong p -type doping in Figs. 10 and 11, respectively. When the material is doped n -type, the defects that have acceptor levels become energetically more favorable, yielding higher concentrations of these defects relative to the intrinsic case. Consistent with this expectation and the fact that the gallium antisite and gallium vacancy possess acceptor levels, we see in Fig. 10 that these are the dominant defects in n -type gallium arsenide. For strongly p -type material, we see in Fig. 11 that the arsenic antisite, a donor, is the only dominant defect species.

At an annealing temperature of 1100 K the Fermi energy for the n -type material varies between 0.77 eV and 0.90 eV, while the Fermi energy for the p -type material varies between 0.18 eV and 0.22 eV, as shown in Fig. 12. Without the compensating effect of the defects, the Fermi energy would be 0.18 eV for the p -type material and very near the conduction band edge for the n -type material. In n -type material, the Fermi energy shows signs of strong compensation across the entire compositional range from gallium rich to arsenic rich, with especially strong compensation closer to the arsenic-rich limit, due to large concentrations of gallium vacancies. In p -type material near the arsenic-rich limit, there is evidence of compensation due to the arsenic antisites.

In n -type material, the gallium vacancy is seen in Fig. 10 to be present in high concentrations, while gallium interstitial concentrations are negligible, falling well below the lower limit of the graph. In p -type GaAs, as seen in Fig. 11, the gallium vacancy occurs in far lower concentrations — around two orders of magnitude lower than gallium interstitial concentrations in the Ga-rich limit. We conclude that Ga interstitials would be likely to play an important role in the diffusion of Ga in p -type, Ga-rich GaAs.

Since equilibrium concentrations of gallium interstitials are still rather low even in the p -type material, we would expect only moderate gallium diffusion rates due to interstitials. Diffusion rates of gallium interstitials may be significantly enhanced if gallium atoms are knocked out of their lattice by ion implantation or irradiation, creating more significant concentrations of gallium interstitials. To quantitatively evaluate the relative contribution of gallium interstitials to gallium diffusion under different experimental conditions, we must compute the barriers for motion between stable configurations of gallium interstitials, which requires us to survey numerous possible migration pathways.

C. Pathways for diffusion

Previously, migration barriers for two low energy migration paths for diffusion of gallium interstitials have been calculated for the +1 and neutral charge states.²⁶ In both cases, an automated procedure was initially used to identify a low energy diffusion path, and the results for the saddle point energy were then converged further. In one case, a low energy path was discovered for a gallium atom to move between the tetrahedral interstitial site between gallium atoms and the tetrahedral interstitial site between arsenic atoms through the connecting hexagonal interstitial site, without entering the lattice network. And in the other case (for the +1 charge state only), a low energy path was discovered for the gallium atom to move from a gallium-arsenic $\langle 111 \rangle$ split interstitial to the tetrahedral interstitial site surrounded by gallium atoms.²⁶ This path can be the second step in the migration of a gallium atom from one tetrahedral site surrounded by gallium atoms to another equivalent tetrahedral site. The first step for this migration would require the gallium atom to reverse this motion, leaving the initial tetrahedral site to form a $\langle 111 \rangle$ gallium-arsenic split

interstitial.

The energy barriers calculated for these two pathways for diffusion in the neutral and +1 charge states were quite similar. The energy barriers calculated by Levasseur-Smith *et al.*²⁶ for migration of a gallium atom from the tetrahedral site surrounded by gallium atoms through the hexagonal site to the tetrahedral site surrounded by arsenic atoms (and on through another hexagonal site to a different tetrahedral site surrounded by gallium atoms) are 1.3 eV for the neutral charge state and 1.4 eV for the +1 charge state. The energy barrier calculated by Levasseur-Smith *et al.*²⁶ for migration of a gallium atom from a tetrahedral site surrounded by gallium atoms through the gallium-arsenic $\langle 111 \rangle$ split interstitial configuration to another tetrahedral interstitial site surrounded by gallium atoms is 1.4 eV (composed of an energy difference of 0.9 eV between the $\langle 111 \rangle$ split interstitial and the tetrahedral interstitial surrounded by gallium atoms and an additional barrier of 0.4 eV to move between these configurations) for the +1 charge state. Levasseur-Smith *et al.* only used their automated procedure to investigate the low energy paths for migration of a gallium atom out of the tetrahedral interstitial configurations (in the neutral and +1 charge states) and the gallium-arsenic $\langle 111 \rangle$ split interstitial configuration (in the +1 charge state), since the other metastable gallium-gallium and gallium-arsenic split interstitial configurations discovered by this group²¹ for the neutral and positive charge states were at least 0.8 eV higher in energy than the tetrahedral interstitial configuration surrounded by gallium atoms.²⁶

Schultz *et al.* identified other metastable gallium interstitial configurations and also calculated the energy barrier for gallium diffusion between tetrahedral interstitial configurations via the non-network path through the hexagonal saddle point in the +1 charge state, obtaining 1.22 eV (1.11 eV) in LDA (PBE) calculations.²⁰ Based on these results for the migration barrier through the hexagonal site and the results of Levasseur-Smith *et al.* for the migration barrier through the gallium-arsenic $\langle 111 \rangle$ split interstitial configuration, together with their calculated formation energies in many charge states for a large number of metastable defects involving insertion of the excess gallium atom into the lattice, Schultz *et al.* predicted that the dominant path for gallium interstitial diffusion in the +1 charge state is likely to be along the non-network path through the hexagonal site, with smaller contributions from in-network paths, and that the migration barriers for the 2+ and 3+ states should be similar to the migration barriers for the 1+ states.²⁰ Given the extent of the survey of defect formation energies available to us, we can now more fully investigate possible low-energy pathways for gallium interstitial diffusion in all the charge states likely to be important for a Fermi level anywhere in the gap.

According to the results presented in Section III A, diffusion of the neutral gallium interstitial via a path through the gallium-gallium $\langle 110 \rangle$ split interstitial configuration may have a lower energy barrier than diffusion along other paths and for other charge states. As we have noted, the increase in energy above the most energetically favorable tetrahedral interstitial is lower for the neutral gallium-gallium $\langle 110 \rangle$ split interstitial than for any other metastable neutral or positively charged gallium split interstitial found in earlier work.^{20,21} Using results of our density functional calculations with norm-conserving pseudopotentials, we found that the formation energy of the metastable neutral gallium-gallium $\langle 110 \rangle$ split interstitial is only 0.53 eV higher than the formation energy calculated for the lowest energy neutral tetrahedral gallium interstitial — this energy difference is 0.57 eV according to the VASP calculations which we used in conjunction with the nudged elastic band method to determine minimum energy diffusion paths and migration barriers, and it is 0.6-0.7 eV according to Schultz *et al.*²⁰ Our discussion in the rest of the paper will be based on the

TABLE I. Uncorrected migration barriers for gallium interstitial diffusion from one tetrahedral position to the nearest neighboring tetrahedral interstitial position, as calculated using the nudged elastic band method.

Charge state	$\langle 110 \rangle$ -split pathway barrier (eV)	hexagonal pathway barrier (eV)
0	0.6	1.2
1+	1.1	1.2
2+	1.0	0.9
3+	0.9	0.7

calculated VASP results for the formation energies and migration barriers.

The initial and middle steps for gallium diffusion between two tetrahedral interstitial sites surrounded by gallium atoms through the gallium-gallium $\langle 110 \rangle$ split interstitial configuration can be seen in Figs. 6(a) and 6(b), respectively. The tetrahedral gallium interstitial atom and the nearest neighbor gallium atom above it and to the right in Fig. 6(a) move a short distance to the right, with a corresponding upward or downward motion, to form the $\langle 110 \rangle$ split pair as seen in Fig. 6(b). The rest of the motion continues the general trend with the right atom of the split interstitial falling into the nearest tetrahedral defect position to the right, while the original gallium interstitial atom moves onto the gallium lattice site beside the new tetrahedral interstitial. The net result is the motion of one gallium atom from the original tetrahedral interstitial site to an equivalent neighboring tetrahedral interstitial site.

We used the nudged elastic band method^{29–32,40,41} to determine the energy barriers for the migration of a gallium atom starting in the tetrahedral gallium interstitial configuration with gallium nearest neighbors, through both the gallium-gallium $\langle 110 \rangle$ split-interstitial pathway and the hexagonal pathway, for the neutral, +1, +2, and +3 charge states. Only the end points (tetrahedral interstitial configurations) were held fixed, and the pathway was allowed to converge freely. The calculated barriers range from 0.6 eV to 1.2 eV, as displayed in Table I. The lowest barrier corresponds to the gallium interstitial passing through the gallium-gallium $\langle 110 \rangle$ split interstitial position in the neutral charge state.

The energy as a function of configuration coordinate for each charge state is shown in Fig. 13 for the complete migration path between two tetrahedral interstitial sites surrounded by gallium atoms passing through the gallium-gallium $\langle 110 \rangle$ split interstitial position. The intermediate point of the fully converged split-interstitial pathway remained at the gallium-gallium $\langle 110 \rangle$ split-interstitial configuration, which can be seen to be a shallow metastable configuration for the neutral charge state. The metastability is visible as a very shallow dip in the curve at the point corresponding to the neutral $\langle 110 \rangle$ split-interstitial configuration (see Fig. 13).

We find that the energy barrier to leave the neutral gallium-gallium $\langle 110 \rangle$ split configuration and continue along the diffusion path is only 0.02 eV, making this defect only barely metastable. This result is in agreement with Schultz *et al.*,²⁰ who find that there is (almost) no barrier for the neutral gallium-gallium $\langle 110 \rangle$ split interstitial to convert to a neutral tetrahedral interstitial surrounded by gallium atoms, and it is in qualitative agreement with Malouin *et al.*,²¹ who do not find the neutral gallium-gallium $\langle 110 \rangle$ split interstitial to be metastable at all.

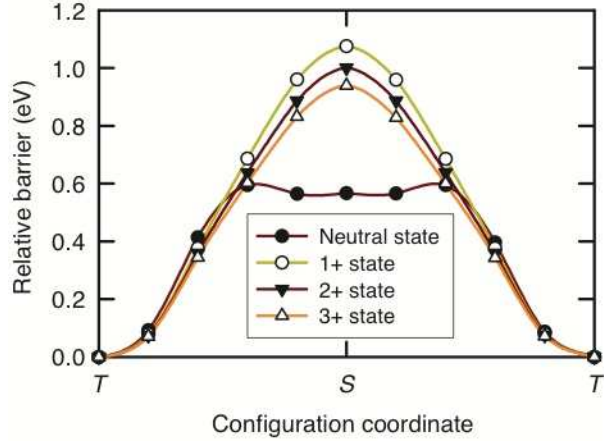


FIG. 13. (Color online) The energy barriers computed with the nudged elastic band method are shown for the migration of a gallium tetrahedral interstitial between gallium atoms (T) to the next-nearest neighboring tetrahedral interstitial position, also between gallium atoms, via the gallium-gallium $\langle 110 \rangle$ split-interstitial position (S), in the neutral, +1, +2, and +3 charge states. The calculated energy at each point along the path is plotted vs. the distance along the path. The energies presented are all energies relative to the formation energy calculated for the tetrahedral interstitial between gallium atoms in the given charge state. The calculations were performed at the points indicated and curves are added to guide the eye.

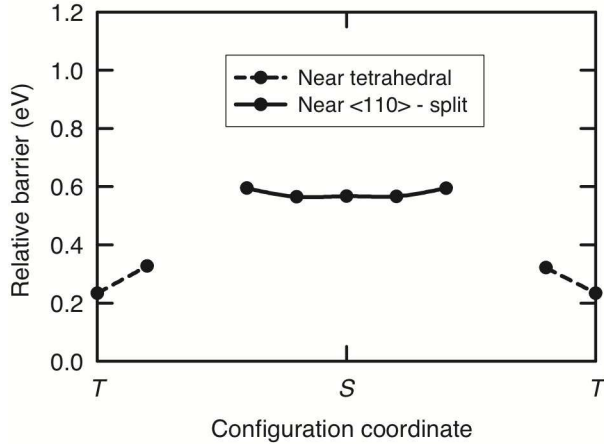


FIG. 14. Corrected energy barriers at 300K are shown for the migration of a neutral gallium tetrahedral interstitial between gallium atoms (T) to the next-nearest neighboring tetrahedral interstitial position, also between gallium atoms, via the gallium-gallium $\langle 110 \rangle$ split-interstitial position (S). The energy at each point along the path is plotted vs. the distance along the path. The energies presented are derived from the nudged elastic band results for the same migration presented in Fig. 13, with a shift of +0.236 eV applied to the neutral tetrahedral part of the calculation, as discussed in the text.

For the +1, +2, and +3 charge states, we find that the gallium-gallium $\langle 110 \rangle$ split interstitial configuration is a saddle point at the midpoint of the diffusion path, as can be seen in Fig. 13, and is therefore unstable. In a slightly different result, Schultz *et al.*²⁰ found enough of a region of metastability to calculate formation energies for the gallium-gallium $\langle 110 \rangle$ split interstitial configuration in these charge states without doing nudged elastic band calculations to investigate diffusion paths that pass through or close to this configuration.

Our results for the energy barriers along this diffusion path for the +1, +2, and +3 charge states, which are just the differences in formation energy between the gallium-gallium $\langle 110 \rangle$ split interstitial and the tetrahedral interstitial surrounded by gallium atoms, are consistent with the results of Schultz *et al.* Schultz *et al.* report the formation energy of the gallium-gallium $\langle 110 \rangle$ split interstitial in the +1 charge state to be 1.12(1.07) eV higher than the formation energy of the tetrahedral interstitial surrounded by gallium atoms, based on their LDA(PBE) calculations.²⁰ This is in good agreement with our calculated energy barrier of 1.1 eV for gallium interstitial diffusion in the +1 charge state between two tetrahedral interstitials surrounded by gallium atoms via the path through the gallium-gallium $\langle 110 \rangle$ split interstitial configuration. Schultz *et al.* report the formation energy of the gallium-gallium $\langle 110 \rangle$ split interstitial in the +2 and +3 charge states to be 0.9-1.0 eV higher than the formation energy of the tetrahedral interstitial surrounded by arsenic atoms.²⁰ Although Schultz *et al.* do not report their results for the +2 and +3 charge states in as much detail or with as much precision as they do for the +1 charge state, we may still make a comparison to our results for the +2 and +3 charge states, by using our results that for these charge states, the formation energies of the two tetrahedral interstitials are very similar, as shown in Fig. 1 and discussed in Section III A. We conclude that the formation energy differences reported by Schultz *et al.* are in reasonable agreement with our calculated energy barriers of 1.0 eV and 0.9 eV for diffusion along this path in the +2 and +3 charge states, respectively.

Since the energy has a simpler dependence on the configuration coordinate for the migration path through the hexagonal interstitial configuration, a figure equivalent to Fig. 13 is not shown for this path. The intermediate point of the fully converged hexagonal pathway between a tetrahedral interstitial site surrounded by gallium atoms and a neighboring tetrahedral interstitial site surrounded by arsenic atoms remained at the hexagonal interstitial configuration. This diffusion path has a single peak in energy at the hexagonal configuration, which is a saddle point for all charge states. The final energy is slightly higher than the initial energy for this migration path, since the gallium begins in the slightly more energetically favorable of the two tetrahedral interstitial configurations and ends in the slightly higher energy configuration. The second step in the migration of a gallium atom via the hexagonal path to a tetrahedral site equivalent to the starting site would be for it to reverse this process, moving from the slightly higher energy tetrahedral interstitial surrounded by arsenic atoms to a neighboring tetrahedral interstitial surrounded by gallium atoms.

As we have discussed in Section III A, the calculated formation energy for any neutral defect with its last electron occupying a shallow hydrogenic bound state composed of conduction band states should be shifted up by a scissors-type correction^{57,58} in order to correctly represent a transition level just below the conduction band edge for the transition from singly positive to neutral. Therefore, as indicated in Section III A, in our calculations of activation energies for diffusion, we shift the formation energy for both neutral tetrahedral interstitials and for the neutral hexagonal interstitial up by the same scissors correction as is needed to shift the effective conduction band edge in our defect calculations up to coincide with the experimental conduction band edge. This correction is 0.236 eV at 300K.

Both the initial and final points as well as the saddle point configuration for the hexagonal path are all shifted up in energy by the same amount for diffusion in the neutral state. Therefore the calculated barrier shown in Table I for diffusion of a neutral gallium interstitial via the hexagonal path is not affected by the scissors correction. However, under conditions where interstitial concentrations are determined by thermal equilibrium, the activation energy for diffusion consists of the formation energy plus the migration barrier for the interstitial. Since the formation energy of the initial neutral tetrahedral interstitial is shifted up, under conditions where interstitial concentrations are determined by thermal equilibrium, the activation energy for neutral gallium interstitial diffusion via the hexagonal path will be increased by the scissors correction.

In the case of neutral interstitial diffusion via the gallium-gallium $\langle 110 \rangle$ split-interstitial path, the scissors correction affects both the formation energy of the initial tetrahedral interstitial and the diffusion barrier. Since the last electron bound to the neutral gallium-gallium $\langle 110 \rangle$ split interstitial occupies a true localized defect state rather than a shallow hydrogenic bound state, the formation energy of this neutral defect configuration should not be shifted up by the scissors correction. Therefore the formation energy of the neutral tetrahedral interstitial configurations which form the initial and final points on this path will be shifted up, while the formation energy of the neutral $\langle 110 \rangle$ split interstitial configuration which forms the midpoint of this path will not. This results in an upward shift of the energy at the initial and final points of this path, relative to the midpoint, by 0.236 eV at 300K.

Fig. 14 shows the corrected energy as a function of configuration coordinate for gallium diffusion via the gallium-gallium $\langle 110 \rangle$ split interstitial pathway in the neutral charge state. The energies are obtained from the nudged elastic band results for the same migration presented in Fig. 13, with a shift of +0.236 eV applied to the neutral tetrahedral interstitial part of the calculation. We have only included points on this graph near the two endpoints and the midpoint — however, there is no evidence to suggest that any more significant additional barrier will develop around the $\langle 110 \rangle$ split interstitial as a result of including corrections to the formation energy of the shallow hydrogenic bound state for the initial and final tetrahedral interstitial configurations. We conclude that the corrected barrier, defined as the difference in energy between the initial configuration and the highest energy configuration along the path, is about 0.35 eV.

For neutral gallium diffusion via the in-network path through the gallium-gallium $\langle 110 \rangle$ split interstitial configuration, the activation energy for diffusion under conditions of thermal equilibrium consists of the formation energy of the initial interstitial configuration (which is shifted up due to the scissors correction) plus the migration barrier (which is shifted down by the same amount). Therefore the activation energy under conditions of thermal equilibrium for gallium diffusion in the neutral state via the gallium-gallium $\langle 110 \rangle$ split interstitial pathway will not be affected by the scissors correction. In fact, the activation energy under conditions of thermal equilibrium for interstitial diffusion via any path is merely the formation energy of the interstitial configuration at the highest energy point in the path — shifting the formation energy of the initial configuration up or down relative to the highest energy configuration does not affect this activation energy.

When we compare the energy barriers for gallium interstitial diffusion through the hexagonal configuration and for gallium interstitial diffusion through the gallium-gallium $\langle 110 \rangle$ split interstitial configuration, we find that the charge state of the diffusing interstitial determines which pathway has the lowest barrier. Calculated diffusion barriers are lower for diffusion of the excess gallium atom through the hexagonal configuration for the $q = +2$ and

+3 charge states, and diffusion barriers are lower for the in-network path involving gallium interstitial diffusion through the gallium-gallium $\langle 110 \rangle$ split interstitial configuration for the neutral and +1 charge states. This suggests that the Fermi level is likely to play a role in determining the relative importance of these two diffusion pathways.

Gallium interstitial diffusion may also proceed through other in-network paths. However, we expect that the dominant contributions to diffusion will be due to the in-network path through the gallium-gallium $\langle 110 \rangle$ split interstitial configuration and the non-network path through the hexagonal site. For the +2 and +3 charge states, the formation energies for all the other metastable split interstitials which have been studied^{20,21} are at least 0.9 eV higher than the formation energy of the tetrahedral interstitial surrounded by gallium atoms. Any additional energy needed to move into and out of these configurations would further raise the energy barrier for diffusion through these configurations. Since the entire energy barrier for diffusion through the hexagonal site is 0.9 eV for the +2 charge state and 0.7 eV for the +3 charge state, according to our calculations, we expect this to be the lowest energy pathway (or at least one of the lowest energy pathways) for diffusion in the +2 and +3 charge states. For the neutral interstitial, the lowest energy non-tetrahedral configuration which has been studied is the gallium-gallium $\langle 110 \rangle$ split interstitial, and there is a negligible additional barrier for moving into and out of this configuration, as discussed above and in Section III A. We conclude that the lowest energy pathway for diffusion in the neutral state will be the pathway through the gallium-gallium $\langle 110 \rangle$ split interstitial. For the +1 charge state, diffusion may proceed through the gallium-arsenic $\langle 111 \rangle$ split interstitial configuration, with a barrier of 1.4 eV, as calculated by Levasseur-Smith *et al.*²⁶ and discussed above, as well as through the gallium-gallium $\langle 110 \rangle$ split interstitial configuration, with a barrier of 1.1 eV, as we have calculated above. We conclude that although both pathways may contribute to diffusion in the +1 charge state, the pathway through the gallium-gallium $\langle 110 \rangle$ split interstitial configuration appears to be the lower energy pathway.

D. Diffusion dependence on stoichiometry and doping

In this section, we combine the calculated defect formation energies and migration barriers in order to get an overall picture of the contribution of gallium interstitials to gallium diffusion in gallium arsenide under different experimental conditions. Because of the dependence of the dominant charge states and the formation energies of defects on the Fermi energy and chemical potential, we examine the contributions due to different defect pathways and different charge states to gallium diffusion as a function of these experimental conditions.

Changes in the chemical potential raise or lower the formation energies of all gallium interstitial configurations by the same amount, since they all involve one excess gallium atom. We have presented the lower and upper limits for the formation energies of gallium interstitials, corresponding to the gallium-rich and arsenic-rich limits, respectively, as a function of the Fermi level in Figs. 1 and 2. Under conditions where interstitial concentrations are determined by thermal equilibrium, changes in the chemical potential will raise or lower the activation energies by the same amount for gallium interstitial diffusion in all charge states and by all pathways. However, changes in the chemical potential do not change the relative importance of different diffusion pathways for the interstitial or diffusion in different charge states. In the following discussion of the effect of the Fermi level on gallium interstitial diffusion, we will focus on diffusion for a chemical potential in the gallium-rich limit.

The experimentally measured Fermi level is determined by many factors, including concentrations of native defects produced by thermal equilibrium or by processes such as irradiation or ion implantation, as well as intentional or unintentional doping. For example, as shown in Section III B, changes in the chemical potential affect the relative concentrations in thermal equilibrium of native defects containing different numbers of excess gallium or arsenic atoms, many of which are charged. Therefore changes in the chemical potential may contribute to changes in the Fermi level.

The dependence of gallium interstitial diffusion on Fermi level is more complicated than its dependence on the chemical potential. In Fig. 15 we display the activation enthalpy for gallium interstitial diffusion in the gallium-rich limit as a function of the Fermi energy for diffusion through the gallium-gallium $\langle 110 \rangle$ split interstitial configuration, under conditions where interstitial concentrations are determined by thermal equilibrium. Activation enthalpies are shown for diffusion via this path for interstitials in each of the four charge states from neutral to triply positive. In this figure as well as all the other figures in this section, results for 300 K are shown: the Fermi energy is shown varying across the 300 K experimental band gap of 1.42 eV.

The activation enthalpy for gallium interstitial diffusion shown in Fig. 15 is the energy required for a gallium tetrahedral interstitial surrounded by gallium atoms to be created and then to migrate through the $\langle 110 \rangle$ gallium-gallium split interstitial position to the next equivalent tetrahedral interstitial position. Fig. 15 shows the activation enthalpy obtained from our VASP calculations, which is the sum of the initial interstitial formation energy and the migration barrier. As discussed in Section III C, this activation enthalpy is equal to the enthalpy of formation of the defect at the highest energy point along the path — in this case, the formation energy of the $\langle 110 \rangle$ gallium-gallium split interstitial. Therefore any uncertainty in the formation energy of the tetrahedral interstitial has no effect on this graph.

Since the activation enthalpy for diffusion via the $\langle 110 \rangle$ gallium-gallium split interstitial path is equal to the formation energy of the $\langle 110 \rangle$ gallium-gallium split interstitial, we may compare our results for this formation energy as obtained in our VASP and our norm-conserving pseudopotential calculations, to see whether these calculations lead to similar results. Fig. 1 in Section III A shows the results of our norm-conserving pseudopotential calculations for the formation energy of the $\langle 110 \rangle$ gallium-gallium split interstitial in its most energetically favorable charge state in the gallium-rich limit, as a function of Fermi energy across the calculated band gap. Although the scissors correction has not been applied to raise the band gap in this figure to its experimental value at 300K, the results of our norm-conserving pseudopotential calculations shown in Fig. 1 may still be compared to the results of our VASP calculations over the range of Fermi levels corresponding to the calculated band gap. The results of our norm-conserving pseudopotential calculations for the formation energy of the $\langle 110 \rangle$ gallium-gallium split interstitial in its most energetically favorable charge state, shown in Fig. 1, are essentially the same as the results of our VASP calculations for the activation enthalpy in the most energetically favorable charge state, shown in Fig. 15.

As we can see in Fig. 15, interstitial diffusion through the $\langle 110 \rangle$ gallium-gallium split interstitial pathway is largely dominated by diffusion in the neutral and +1 states. The activation enthalpy for diffusion via this pathway is lowest for diffusion in the neutral and +1 charge states across much of the available range of Fermi energies. Only in highly *p*-doped material, with a Fermi level approaching the valence band edge, are the activation enthalpies for diffusion in the +2 and +3 charge states as low or lower than the activation enthalpy for diffusion in the +1 state.

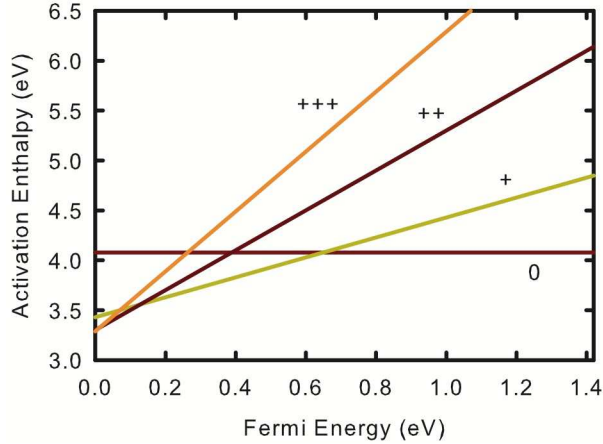


FIG. 15. (Color online) The activation enthalpy for diffusion through the $\langle 110 \rangle$ gallium-gallium split interstitial configuration for charge states from neutral to +3, as a function of Fermi energy ϵ_F , in the gallium-rich limit, under conditions where interstitial concentrations are determined by thermal equilibrium.

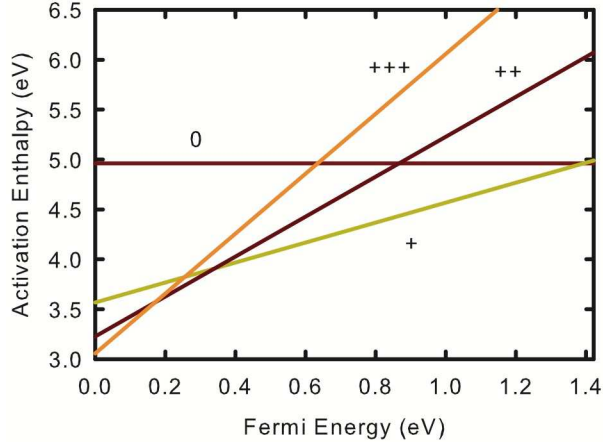


FIG. 16. (Color online) The activation enthalpy for diffusion through the hexagonal interstitial position for charge states from neutral to +3, as a function of Fermi energy ϵ_F , in the gallium-rich limit, under conditions where interstitial concentrations are determined by thermal equilibrium.

In Fig. 16 we display a similar graph for the case in which the tetrahedral gallium interstitial migrates from its location between gallium atoms to the nearest tetrahedral location between arsenic atoms via the hexagonal opening in the lattice between the two tetrahedral locations. Again, we note that the activation enthalpy presented in this graph is just the formation energy of the defect at the highest energy point along the path. The highest energy point along the path shown in Fig. 16 corresponds to the hexagonal interstitial; therefore changes in the formation energy of the initial and final tetrahedral interstitials do not affect this graph.

Since the activation enthalpy for diffusion via the hexagonal interstitial path is equal to the formation energy of the hexagonal interstitial, we may compare the results of our

norm-conserving pseudopotential calculations for the formation energy of the hexagonal interstitial to the results of our VASP calculations for the activation enthalpy for gallium interstitial diffusion through the hexagonal position. Fig. 1 in Section III A shows the results of our norm-conserving pseudopotential calculations for the formation energy of the hexagonal interstitial in its most energetically favorable charge state in the gallium-rich limit, as a function of Fermi energy across the calculated band gap. These results are essentially the same as the results of our VASP calculations for the activation enthalpy in the most energetically favorable charge state, shown in Fig. 16.

Comparison of Figs. 15 and 16 suggests that diffusion can be modeled more simply for high and mid-gap Fermi energies than it can be for Fermi energies near the valence band edge. These figures show that the neutral and +1 charge states are the most energetically favorable charge states for diffusion via the split interstitial and hexagonal pathways over most of the range of possible Fermi energies, except for Fermi energies near the valence band edge. We also observe that activation energies are lower for diffusion via the split interstitial pathway than for diffusion via the hexagonal pathway for both the neutral and the +1 charge states. We conclude that diffusion proceeds primarily through the in-network path through the $\langle 110 \rangle$ gallium-gallium split interstitial configuration in the neutral and +1 charge states over most of the range of possible Fermi energies, except for Fermi energies near the valence band edge. Diffusion is most energetically favorable in the neutral charge state for Fermi energies around midgap and above. Diffusion is most energetically favorable in the +1 charge state for Fermi energies between mid-gap and the region near the valence band edge. For Fermi energies where the +1 charge state dominates diffusion, overall diffusion may be enhanced by small additional contributions to diffusion in this charge state by the hexagonal pathway and the pathway through the $\langle 111 \rangle$ gallium-arsenic split interstitial configuration, which was explored by Levasseur-Smith *et al.*²⁶ and discussed above in Section III C.

We find that gallium interstitial diffusion should be the most complicated to model and also the most rapid for Fermi energies near the valence band edge, when concentrations of interstitials are determined by thermal equilibrium. Figs. 15 and 16 show that the activation enthalpies in the most energetically favorable charge state for both the $\langle 110 \rangle$ gallium-gallium split interstitial path and the hexagonal path are lowest when the Fermi energy is low. This should result in more rapid diffusion via these paths under conditions of *p*-type doping. The most energetically favorable diffusion for Fermi energies below about 0.2 eV is diffusion in the +2 or +3 charge state via the hexagonal pathway. However, no single charge state can be said to dominate diffusion for a Fermi energy with 0.2 eV of the valence band edge, as activation energies for diffusion in the +1 and +2 charge states are very similar at the upper end of this range, and activation energies for diffusion in the +2 and +3 charge states are very similar as the Fermi energy approaches the valence band edge. This can lead to a complicated diffusion profile, and difficulties extending models for diffusion which have worked well for higher Fermi energies into this region.

Fig. 17 shows the lowest activation enthalpies for diffusion via either the hexagonal path or the $\langle 110 \rangle$ gallium-gallium split interstitial path in the gallium-rich limit, as a function of the Fermi energy across the experimental 300 K band gap, for diffusion when interstitial concentrations are determined by thermal equilibrium. In the +2 and +3 charge states, the lowest activation enthalpy involves diffusion via the hexagonal defect pathway. In the +1 and neutral charge states, the lowest activation enthalpy involves diffusion via the split interstitial pathway. As shown in Fig. 17, the lowest activation enthalpy for diffusion when interstitial concentrations are determined by thermal equilibrium is 3.1 eV in the gallium-

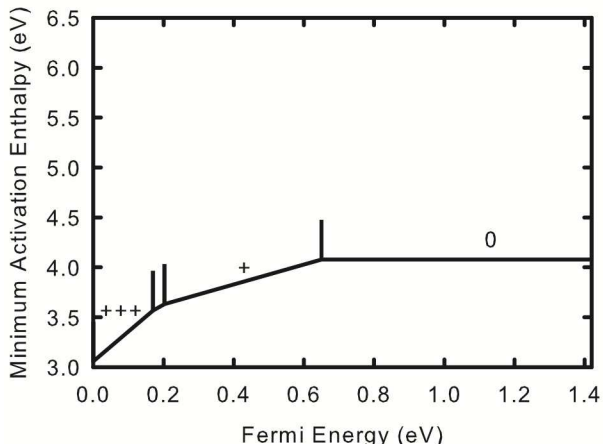


FIG. 17. The minimum activation enthalpy for gallium interstitial diffusion via the pathways calculated in this paper as a function of Fermi energy ϵ_F , in the gallium-rich limit, under conditions where interstitial concentrations are determined by thermal equilibrium. In the +2 and +3 charge states, migration through the hexagonal configuration possesses the lowest activation enthalpy. In the neutral and +1 charge states, migration through the $\langle 110 \rangle$ split interstitial configuration possesses the lowest activation enthalpy.

rich limit, corresponding to diffusion via the hexagonal path in the +3 charge state. Under arsenic-rich conditions, due to the larger energy cost for forming gallium interstitials, the activation enthalpies at all Fermi energies are increased by 0.5 eV.

If gallium interstitials have been formed through damage associated with implantation, radiation, or processing, then we may consider migration starting from an abundance of non-equilibrium interstitials in the material. These pre-existing interstitials are mostly present in their lowest energy charge state, which depends on the Fermi energy, but they may diffuse primarily in a different charge state which has a lower migration barrier. In this case, the activation energy for diffusion to occur in a given charge state is the energy it takes to promote the pre-existing defect to this charge state from the lowest energy charge state, plus the migration barrier for the given charge state. These activation energies are plotted as a function of Fermi energy in Fig. 18 and Fig. 19 for the $\langle 110 \rangle$ gallium-gallium split interstitial pathway and the hexagonal pathway, respectively.

As can be seen by comparing Figs. 18 and 19 to the corresponding figures for diffusion when interstitial concentrations are determined by thermal equilibrium, Figs. 15 and 16, the presence of non-equilibrium concentrations of interstitials does not affect which pathway and charge state has the lowest activation energy for diffusion for a given Fermi energy. Regardless of whether we consider the existing interstitial concentrations to be in thermal equilibrium or out of equilibrium, we conclude that diffusion proceeds primarily via the in-network path through the $\langle 110 \rangle$ gallium-gallium split interstitial configuration in the neutral charge state for Fermi energies around midgap and above, and via the same path in the +1 charge state for Fermi energies between mid-gap and the region near the valence band edge. Similarly, we conclude that diffusion via the hexagonal path in the +2 and +3 charge states becomes the most energetically favorable for Fermi energies within 0.2 eV of the valence band edge. As in the case when interstitial concentrations are determined by thermal equilibrium, no single charge state can be said to dominate diffusion for a Fermi energy within 0.2 eV of

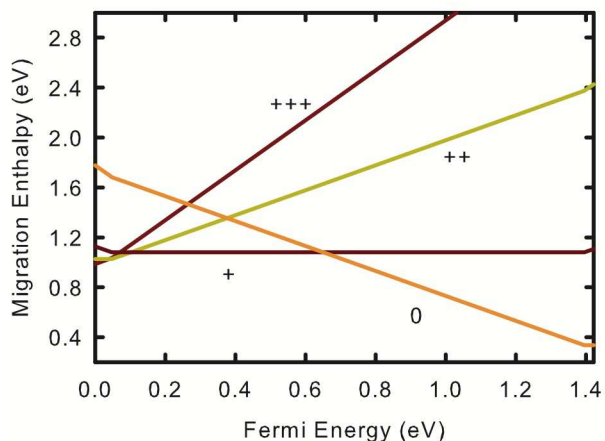


FIG. 18. (Color online) The energy needed for a pre-existing gallium tetrahedral interstitial between Ga atoms to change from the minimum energy charge state to the charge state specified and then migrate to another tetrahedral site, passing through the $\langle 110 \rangle$ gallium-gallium split interstitial configuration, is plotted as a function of ϵ_F .

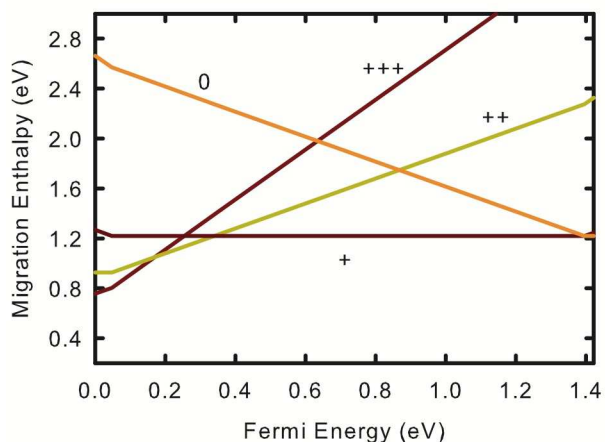


FIG. 19. (Color online) The energy needed for a pre-existing gallium tetrahedral interstitial between Ga atoms to change from the minimum energy charge state to the charge state specified and then migrate to another tetrahedral site, passing through the hexagonal gallium interstitial configuration, is plotted as a function of ϵ_F .

the valence band edge, as activation energies for diffusion in the +1 and +2 charge states are very similar at the upper end of this range, and activation energies for diffusion in the +2 and +3 charge states are very similar as the Fermi energy approaches the valence band edge.

However the activation energy for interstitial diffusion is larger when non-equilibrium concentrations of pre-existing interstitials are not available. The activation energy for diffusion when interstitial concentrations are determined by thermal equilibrium is equal to the activation energy for diffusion when there are non-equilibrium concentrations of pre-existing

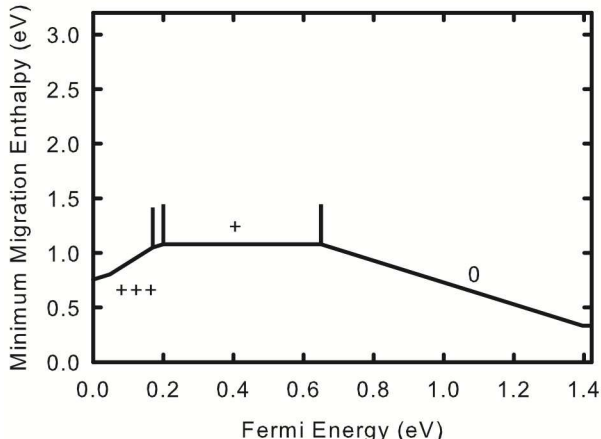


FIG. 20. The minimum activation enthalpy for gallium interstitial diffusion via the pathways calculated in this paper as a function of Fermi energy ϵ_F , in the gallium-rich limit, under conditions where there are non-equilibrium concentrations of pre-existing interstitials. In the +2 and +3 charge states, migration through the hexagonal configuration possesses the lowest activation enthalpy. In the neutral and +1 charge states, migration through the $\langle 110 \rangle$ split interstitial configuration possesses the lowest activation enthalpy.

interstitials plus the additional formation energy needed to create an interstitial in its lowest energy configuration and charge state at the given Fermi energy.

Fig. 20 shows the lowest activation enthalpies for diffusion via either the hexagonal path or the $\langle 110 \rangle$ gallium-gallium split interstitial path in the gallium-rich limit, as a function of the Fermi energy across the experimental 300 K band gap, for diffusion when there are non-equilibrium concentrations of pre-existing interstitials. As for the case when interstitial concentrations are determined by thermal equilibrium, in the +2 and +3 charge states, the lowest activation enthalpy involves diffusion via the hexagonal defect pathway. In the +1 and neutral charge states, the lowest activation enthalpy involves diffusion via the split interstitial pathway.

We conclude from the results shown in Fig. 20 that if there are non-equilibrium concentrations of pre-existing interstitials, gallium interstitial diffusion will be somewhat enhanced by strong p -type doping, and greatly enhanced by strong n -type doping. As in the case where interstitial concentrations are determined by thermal equilibrium, we see in Fig. 20 that the activation enthalpy for diffusion is reduced as the Fermi level approaches the valence band edge. This is due to the low barrier of 0.7 eV for diffusion via the hexagonal path in the +3 charge state, which should result in enhanced diffusion when lower Fermi levels make it more likely for any existing interstitials to be present in this charge state. However, in contrast to the behavior we see when interstitial concentrations are determined by thermal equilibrium, if there are non-equilibrium concentrations of pre-existing interstitials, we see that the activation enthalpy for diffusion is reduced considerably more as the Fermi level approaches the conduction band edge. This is due to the even lower barrier of 0.35 eV for diffusion via the split interstitial path in the neutral charge state, which should result in greatly enhanced gallium interstitial diffusion when Fermi levels approaching the conduction band edge make it more likely for any existing interstitials to be present in the neutral charge state.

Comparison to experimental results requires that we take into account the fact that both gallium interstitials and gallium vacancies may contribute to gallium diffusion in gallium arsenide. Modeling of experimental results, as reviewed in,² has often been used to help identify the dominant contributor to gallium diffusion. As a result of this modeling, the gallium vacancy has been identified as the most likely agent for gallium diffusion for intrinsic and n -type doping, while the gallium interstitial has been identified as the most likely agent for gallium diffusion for heavy p -type doping.² To determine the circumstances under which interstitials or vacancies dominate gallium diffusion theoretically, we must compare the activation enthalpies across the ranges of doping from p -type to n -type and composition from gallium rich to arsenic rich.

For the contributions to gallium diffusion due to gallium vacancies, we will focus on diffusion involving the simple gallium vacancy. A more complicated equivalent defect, consisting of a complex of an arsenic vacancy and an arsenic antisite, has been identified as having a lower formation energy than the simple gallium vacancy for Fermi energies less than 0.3 eV above the valence band edge.^{20,22} However it is difficult to envision a low-energy gallium diffusion pathway which primarily involves this complex. A second-neighbor hop of a diffusing gallium atom from a gallium lattice site into a gallium vacancy has the net effect of moving the gallium vacancy in the opposite direction, without creating any further defects. However, if a diffusing gallium atom moves into the arsenic vacancy part of the arsenic vacancy-arsenic antisite complex, this produces a complex consisting of a pair of antisites. Further movement of the entire $\text{Ga}_{\text{As}}\text{-As}_{\text{Ga}}$ complex would not lead to any further net motion of gallium. Even in strongly p -type gallium arsenide, where the arsenic vacancy-arsenic antisite complex should be somewhat more numerous than the simple gallium vacancy, the average distance between these complexes will be considerably further than a second-neighbor distance. Movement of a diffusing gallium atom between the arsenic vacancies in these complexes would require the diffusing atom to come out of the vacancy and diffuse a significant distance as an interstitial before finding another arsenic or gallium vacancy.

There is basic agreement on the general picture of gallium vacancies obtained from theoretical calculations and experimental results. Our calculated formation energies for simple gallium vacancies appear in Figs. 1 and 2 for the gallium-rich limit and the arsenic-rich limit, respectively. We find that the energetically preferred charge states of the simple gallium vacancy range from neutral to -3 , as a function of the Fermi level, in general agreement with previous calculations.^{14,20,23,62–65} In agreement with this theoretical picture, charge states of the gallium vacancy which have been used in the modeling of gallium diffusion range from triply negative for n -type to singly negative for p -type.² A positron annihilation experiment is consistent with the gallium vacancy existing in the triply negative charge state in n -type material.⁶⁶

Energy barriers for diffusion of the gallium vacancy have been calculated by two theoretical groups. Bockstedte and Scheffler²² identified the diffusion pathway as a second neighbor hop, with a barrier of 1.7 eV in the neutral charge state and 1.9 eV in the triply negative charge state. Subsequently El-Mellouhi and Mousseau²⁴ identified another second-neighbor hop (different in the details) to be the lowest-energy pathway for gallium vacancy diffusion, with energy barriers of 1.7, 1.7, 1.84, and 2.0 eV in the neutral, singly negative, doubly negative, and triply negative charge states, respectively. As discussed above, these are the most energetically favorable charge states of the simple gallium vacancy for a Fermi level anywhere in the gap. We have used the energy barriers for gallium vacancy diffusion cal-

culated by El-Mellouhi and Mousseau²⁴ when calculating activation enthalpies for gallium vacancy diffusion.

All the calculated diffusion barriers for gallium vacancies are larger than all the calculated diffusion barriers for gallium interstitials, for defects in any of the dominant charge states across the possible range of Fermi energies. Therefore activation enthalpies for diffusion will be larger for pre-existing, non-equilibrium concentrations of vacancies than for similar pre-existing concentrations of interstitials. Irradiation may knock gallium atoms far enough from their lattice sites to leave behind separate vacancy-rich and interstitial-rich regions. Due to the lower activation enthalpies for diffusion of pre-existing gallium interstitials, we may expect more rapid gallium diffusion in the interstitial-rich regions than in the vacancy-rich regions in irradiated GaAs.

For the case when concentrations of defects are determined by thermal equilibrium, we calculated the activation enthalpies for gallium vacancy diffusion using our numbers for formation energies and the barriers calculated by El-Mellouhi and Mousseau,²⁴ listed above. We find that the vacancy will be the dominant agent in gallium diffusion for *n*-type gallium arsenide across the entire range of chemical potentials from gallium-rich to arsenic-rich. For example, for a Fermi level 0.8 eV above the valence band edge, the activation enthalpy for vacancy diffusion in the most favorable charge state is 0.9 eV (1.9 eV) lower than the activation enthalpy for interstitial diffusion in the most favorable charge state in the gallium-rich (arsenic-rich) limit. The charge state of the gallium vacancy which dominates diffusion under these conditions is triply negative.

For *p*-type GaAs with defect concentrations determined by thermal equilibrium, we find that the relative contributions of vacancies and interstitials to gallium diffusion are more dependent on the stoichiometry. For example, in the gallium-rich limit, for a Fermi level 0.2 eV above the valence band edge, the activation enthalpy for interstitial diffusion in the most favorable charge state is 1.2 eV lower than the activation enthalpy for vacancy diffusion in the most favorable charge state. In the arsenic-rich limit, for the same Fermi level, the activation enthalpies for interstitial and vacancy diffusion are essentially the same (the activation enthalpy is 0.1 eV lower for interstitial diffusion than for vacancy diffusion). We conclude that for a Fermi level 0.2 eV above the valence band edge, interstitials dominate diffusion in gallium-rich gallium arsenide, while both interstitials and vacancies make significant contributions to diffusion in arsenic-rich gallium arsenide.

The complete picture we have developed for gallium diffusion in gallium arsenide across the full ranges of Fermi level and stoichiometry can allow us to resolve an apparent disagreement between the models obtained by fitting some of the experiments described in Section I. First, we note that gallium diffusion in gallium-rich material will involve gallium interstitials in the the +1 and neutral charge states when near intrinsic doping conditions and in the +3 and +2 charge states when doping is heavily *p*-type, according to our results as shown in Fig. 17. For example, we may consider an experiment where diffusion occurs at an annealing temperature of 1100 K. We self-consistently evaluated the defect concentrations as discussed in Section III B, and found that the Fermi energy is about 0.6 eV under intrinsic conditions at 1100 K. At this Fermi level, we find that the +1 charge state of the interstitial will have the lowest activation enthalpy for diffusion, with the neutral state being energetically competitive.

In recent experiments on zinc-gallium co-diffusion into gallium arsenide resulting in low concentrations of zinc, the authors conclude from continuum model fits that the neutral and +1 charge states of gallium interstitials will be the most significant interstitials involved in

gallium diffusion.^{3,9} Our calculations are consistent with this conclusion for low concentrations of zinc, since this material is not heavily *p*-doped. The authors also note that their model was unable to properly fit the diffusion profiles for gallium-rich gallium arsenide in regions with higher concentrations of zinc.^{3,9} This is not surprising, since we would expect more highly charged interstitials to contribute more significantly than the neutral and +1 charged interstitials and the gallium vacancies which were included in the model in gallium-rich, highly *p*-doped material.

Earlier experiments that indicated that the more highly positively charged states (+2 and +3) of gallium interstitials are the most important charge states for diffusion, on the other hand, were prepared with more significant concentrations of *p*-type dopants.^{2,6,7,67} Our calculations support this conclusion as well, because this material was prepared under the more heavily *p*-doped conditions which favor gallium interstitial diffusion in the +2 or +3 charge states. The authors of one of these papers noted that there were difficulties involved in using +2 charged gallium interstitials to properly fit the diffusion profiles in the regions with low concentrations of dopants, and that the solution to these difficulties would probably involve the use of +1 charged interstitials in the model, in addition to +2 and +3 charged interstitials.⁶

Taking into account all these experimental results and the results of our calculations, we see that many details of the preparation of the material must be known in order to correctly predict which defects and charge states should be included when modeling the material. Local doping, stoichiometry, and any non-equilibrium defect concentrations all can play a role in determining what should go into the model.

IV. CONCLUSION

In this investigation, the formation enthalpies, structural properties, and activation enthalpies for diffusion of gallium interstitials in gallium arsenide across the entire range of chemical potentials from the arsenic-rich limit to the gallium-rich limit and across the range of doping level from *p*-type to *n*-type were examined. Activation enthalpies for diffusion were calculated both for conditions where interstitial concentrations are determined by thermal equilibrium, and for material containing pre-existing, non-equilibrium concentrations of interstitials. Regions with substantial non-equilibrium concentrations of interstitials may be present in material which has been irradiated.

From comparisons to published results for energy barriers for diffusion of gallium vacancies, it was shown that gallium vacancies in the triply negative charge state will dominate diffusion in *n*-type material, that both gallium interstitials and gallium vacancies can be important agents for gallium diffusion in material that is *p*-type and arsenic rich, and that gallium interstitials in singly, doubly, and triply positive charge states will dominate diffusion in gallium-rich gallium arsenide with various levels of *p*-type doping.

The results presented in this paper demonstrate that the complete picture for diffusion of gallium in gallium arsenide is sensitive to the both the stoichiometry and doping of the material and involves a variety of defects, migration pathways, and charge states across the accessible ranges of doping and stoichiometry. The general picture we have obtained can offer guidance on which defects and charge states should be considered for successful modeling of gallium diffusion, and which can be ignored, depending on the details of the experiment. For example, these results allow confirmation with microscopically based theory that in bulk modeling of gallium diffusion it is essential to include doubly and triply positive

gallium interstitials for strongly p -doped, gallium-rich gallium arsenide; however it may be acceptable only to consider the singly positive charge state of the gallium interstitial when the doping level is closer to intrinsic than strongly p -doped, especially if the material is not gallium-rich.

ACKNOWLEDGMENTS

The authors are grateful for support from the Air Force Office of Scientific Research for grants of computer time at computing centers located at AFRL, ARL, NAVO, and ERDC under DOD HPCMO Project No. AFOSR11693MO1. Some of the preliminary work was done with support from the Air Force Office of Scientific Research under Grants No. F49620-96-1-0167 and F49620-97-1-0479, and additional grants for computer time at the NSF/NPACI Supercomputing Centers at SDSC and TACC and on the Wayne State University Grid. And one author (JTS) gratefully acknowledges enlightening discussion with H. Bracht.

* joseph.schick@villanova.edu

- ¹ H. Mehrer, "Diffusion in solids," (Springer-Verlag, 2007).
- ² T. Y. Tan, U. Gösele, and S. Yu, *Crit. Rev. in Sol. State and Mater. Sci.* **17**, 47 (1991).
- ³ H. Bracht and S. Brotzmann, *Phys. Rev. B* **71**, 115216 (2005).
- ⁴ S. Koumetz, J. C. Pesant, and C. Dubois, *J. Phys. Condens. Matter* **18**, L283 (2006).
- ⁵ E. P. Zucker, A. Hashimoto, T. Fukunaga, and N. Watanabe, *Appl. Phys. Lett.* **54**, 564 (1989).
- ⁶ G. Bösker, N. A. Stolwijk, H.-G. Hettwer, A. Rucki, W. Jäger, and U. Södervall, *Phys. Rev. B* **52**, 11927 (1995).
- ⁷ G. Bösker, N. A. Stolwijk, H. Mehrer, U. Södervall, and W. Jäger, *Journal of Applied Physics* **86**, 791 (1999).
- ⁸ H. Bracht, M. S. Norseng, E. E. Haller, and K. Eberl, *Physica B* **308-310**, 831 (2001), ISSN 0921-4526.
- ⁹ H. Bracht, private communication.
- ¹⁰ S. B. Zhang and J. E. Northrup, *Phys. Rev. Lett.* **67**, 2339 (1991).
- ¹¹ D. J. Chadi, *Phys. Rev. B* **46**, 15053 (1992).
- ¹² D. J. Chadi, *Phys. Rev. B* **46**, 9400 (1992).
- ¹³ J. I. Landman, C. G. Morgan, J. T. Schick, P. Papoulias, and A. Kumar, *Phys. Rev. B* **55**, 15581 (1997).
- ¹⁴ J. T. Schick, C. G. Morgan, and P. Papoulias, *Phys. Rev. B* **66**, 195302 (2002).
- ¹⁵ Y. Bar-Yam and J. D. Joannopoulos, *Phys. Rev. B* **30**, 1844 (1984).
- ¹⁶ S. Pantelides, I. Ivanov, M. Scheffler, and J. Vigneron, *Physica B & C* **116**, 18 (1983), ISSN 0378-4371.
- ¹⁷ R. J. Needs, *Journal of Physics: Condensed Matter* **11**, 10437 (1999)
- ¹⁸ S. Goedecker, T. Deutsch, and L. Billard, *Phys. Rev. Lett.* **88**, 235501 (May 2002).
- ¹⁹ M. J. Puska, S. Pöykkö, M. Pesola, and R. M. Nieminen, *Phys. Rev. B* **58**, 1318 (1998).
- ²⁰ P. A. Schultz and O. A. von Lilienfeld, *Modelling and Simulation in Materials Science and Engineering* **17**, 084007 (2009).
- ²¹ M.-A. Malouin, F. El-Mallouhi, and N. Mousseau, *Phys. Rev. B* **76**, 045211 (2007).

- ²² M. Bockstedte and M. Scheffler, Z. Phys. Chem. (Munich) **200**, 195 (1997).
- ²³ F. El-Mellouhi and N. Mousseau, Phys. Rev. B **71**, 125207 (2005).
- ²⁴ F. El-Mellouhi and N. Mousseau, Phys. Rev. B **74**, 205207 (2006).
- ²⁵ P. G. Papoulias, C. G. Morgan, and J. T. Schick, submitted(2011); P. G. Papoulias, Ph.D. thesis, Wayne State University (2009).
- ²⁶ K. Levasseur-Smith and N. Mousseau, J. Appl. Phys. **103**, 113502 (2008).
- ²⁷ K. Levasseur-Smith and N. Mousseau, Eur. Phys. J. B **64**, 165 (2008).
- ²⁸ M. Bockstedte, A. Kley, J. Neugebauer, and M. Scheffler, Comput. Phys. Commun. **107**, 187 (1997).
- ²⁹ G. Kresse and J. Hafner, Phys. Rev. B **47**, 558 (Jan 1993).
- ³⁰ G. Kresse, Ph.D. thesis, Technische Universität Wien (1993).
- ³¹ J. F. G. Kresse, Comput. Mat. Sci. **6**, 15 (1996).
- ³² G. Kresse and J. Furthmüller, Phys. Rev. B **54**, 11169 (Oct 1996).
- ³³ P. Hohenberg and W. Kohn, Phys. Rev. **136**, B864 (1964).
- ³⁴ D. M. Ceperley and G. J. Alder, Phys. Rev. Lett. **45**, 566 (1980).
- ³⁵ J. Perdew and A. Zunger, Phys. Rev. B **23**, 5048 (1981).
- ³⁶ L. Kleinman and D. M. Bylander, Phys. Rev. Lett. **48**, 1425 (1982).
- ³⁷ D. R. Hamann, Phys. Rev. B **40**, 2980 (1989).
- ³⁸ D. Vanderbilt, Phys. Rev. B **41**, 7892 (Apr 1990).
- ³⁹ G. Kresse and J. Hafner, J. Phys. Condens. Mat. **6**, 8245 (1994).
- ⁴⁰ H. Jónsson, G. Mills, and K. W. Jacobsen, “Classical and quantum dynamics in condensed phase systems,” (World Scientific, 1998) Chap. 16, pp. 385–404.
- ⁴¹ G. Mills, H. Jónsson, and G. K. Schenter, Surf. Sci. **324**, 305 (1995).
- ⁴² F. D. Murnaghan, Proc. Natl. Acad. Sci. **30**, 244 (1944).
- ⁴³ J. S. Blakemore, J. Appl. Phys. **53**, R123 (1982).
- ⁴⁴ K. Momma and F. Izumi, J. Appl. Crystallog. **41**, 653 (2008).
- ⁴⁵ A. F. Kohan, G. Ceder, D. Morgan, and C. G. Van de Walle, Phys. Rev. B **61**, 15019 (2000).
- ⁴⁶ G. Makov and M. C. Payne, Phys. Rev. B **51**, 4014 (1995).
- ⁴⁷ C. G. Van de Walle and J. Neugebauer, J. Appl. Phys. **95**, 3851 (April 2004).
- ⁴⁸ C. Freysoldt, J. Neugebauer, and C. G. Van de Walle, Phys. Rev. Lett. **102**, 016402 (2009).
- ⁴⁹ R. M. Nieminen, Topics Appl. Physics **104**, 29 (2007).
- ⁵⁰ G. A. Baraff and M. Schlüter, Phys. Rev. Lett. **55**, 2340 (1985).
- ⁵¹ G. A. Baraff and M. Schlüter, Phys. Rev. B **33**, 7346 (1986).
- ⁵² Differences in the formation energies presented here and our previously published calculations¹⁴ are a result of having now evaluated the bulk arsenic structure within our own computations, rather than relying upon a previous calculation that used the same codes. This brings our formation energies into closer agreement with other work. For example, the neutral arsenic antisite formation energy in the arsenic-rich limit was stated to be 1.8 eV in our earlier work, and with the updated bulk arsenic formation energy it is now 1.3 eV, which agrees with the calculation due to Schultz *et al.*²⁰ to within the expected precision of density functional theory.
- ⁵³ S. Lany and A. Zunger, Phys. Rev. B **78**, 235104 (2008).
- ⁵⁴ P. A. Schultz, Phys. Rev. Lett. **96**, 246401 (2006).
- ⁵⁵ B. R. Tuttle and S. T. Pantelides, Phys. Rev. Lett. **101**, 089701 (2008).
- ⁵⁶ P. A. Schultz, Phys. Rev. Lett. **101**, 089702 (2008).
- ⁵⁷ G. A. Baraff and M. Schlüter, Phys. Rev. B **30**, 1853 (1984).
- ⁵⁸ K. A. Johnson and N. W. Ashcroft, Phys. Rev. B **58**, 15548 (1998).

- ⁵⁹ H. J. Monkhorst and J. D. Pack, Phys. Rev. B **13**, 5188 (1976).
- ⁶⁰ A. Becke and K. Edgecombe, J. Chem. Phys. **92**, 5397 (1990).
- ⁶¹ R. Wyckoff, *Crystal Structures, Second Edition* (Wiley, New York, 1963).
- ⁶² G. A. Baraff and M. Schlüter, Phys. Rev. Lett. **55**, 1327 (1985).
- ⁶³ J. E. Northrup and S. B. Zhang, Phys. Rev. B **47**, 6791 (1993).
- ⁶⁴ I. Gorczyca, N. E. Christensen, and A. Svane, Phys. Rev. B **66**, 075210 (2002).
- ⁶⁵ A. Janotti, S.-H. Wei, S. B. Zhang, S. Kurtz, and C. G. Van de Walle, Phys. Rev. B **67**, 161201 (2003).
- ⁶⁶ J. Gebauer, R. Zhao, P. Specht, E. R. Weber, F. Borner, F. Redmann, and R. Krause-Rehberg, Appl. Phys. Lett. **79** (2001).
- ⁶⁷ S. Yu, T. Y. Tan, and U. Gösele, J. Appl. Phys. **69**, 3547 (1991).